Cell size regulation in bacteria: a tale of old regulators with new mechanisms

Ezza Khan and Paola E. Mera*

Department of Microbiology, University of Illinois at Urbana-Champaign, Urbana, IL, USA

* Corresponding author e-mail address: pmera@illinois.edu

SUMMARY

Proper function in a bacterial cell relies on intrinsic cell size regulation. The molecular mechanisms underlying how bacteria maintain their cell size remain unclear. The conserved regulator DnaA, the initiator of chromosome replication, is associated to size regulation by controlling the number of origins of replication (*oriC*) per cell. In this study, we identify and characterize a new mechanism in which DnaA modulates cell size independently of *oriC*-copy number. By altering the levels of DnaA without impacting chromosome replication, we demonstrate that DnaA's activity as a transcription factor can slow down cell elongation rate resulting in cells that are ~20% smaller. We identify the peptidoglycan biosynthetic enzyme MurD as a key player of cell size regulation in *Caulobacter crescentus* and in the evolutionarily distant bacterium *Escherichia coli*. Collectively, our findings provide mechanistic insights to the complex regulation of cell size in bacteria.

KEY WORDS. Cell size, DnaA, peptidoglycan, MurD, elongation rate, cytokinesis, *C. crescentus, E. coli*, ppGpp, FtsZ

INTRODUCTION

Across species, bacteria display a diversity of cell shapes, yet within each species, there is a remarkable uniformity in both shape and size (Young, 2006). Maintaining cell size regulation is fundamental for the ability of bacteria to perform basic physiological functions, such as surface transport, biosynthesis, proteome regulation, chromosomal maintenance, and nutrient exchange (Ho & Amir, 2015). For instance, when a cell becomes too large, nutrient transport/utilization can be impacted as transport within the cell is dependent on diffusion (Beveridge, 1988; (Amir, 2014; Grant et al., 2021; Willis & Huang, 2017). Similarly, if a cell becomes too small, it lacks essential volume needed for housekeeping maintenance that can jeopardize the ability to properly segregate their chromosomes (Beveridge, 1988; Willis & Huang, 2017). Regulation of size and shape have also been found to impact virulence (Bartlett et al., 2017; Dalia & Weiser, 2011; Lenski & Travisano, 1994; Salama, 2020; Taylor et al., 2019). *Streptococcus pneumoniae's* ability to reduce its size helps this pathogenic bacterium to circumvent the host immune system (Dalia & Weiser, 2011). Although cell size regulation in bacteria has been intensively studied, the molecular mechanisms involved remain still quite limited.

Bacteria modulate their cell size while orchestrating numerous molecular machineries that temporally and spatially coordinate the replication and segregation of the chromosome with the elongation and constriction of the cell envelope (Westfall & Levin, 2017). One of the conserved regulators of the cell cycle that has been implicated in cell size regulation is the chromosome replication initiator protein, DnaA. DnaA regulates the number of origins of replication (*oriC*) per cell in response to nutrient availability (Boye et al., 1996; Hallgren & Jonas, 2024; Lobner-Olesen et al., 1989). Cells grown in nutrient rich medium (fast growth rates) initiate new rounds of chromosome replication within shorter time intervals and become larger in size compared to cells grown in minimal media (slower growth rates) (Cooper & Helmstetter, 1968; Donachie, 1968). The positive correlation between cell size and *oriC* copy number were reported ~½ century ago (Cooper & Helmstetter, 1968; Donachie, 1968; Helmstetter et al., 1968; Yoshikawa et al., 1964). Since then, many studies have been reported supporting and rejecting the role of chromosome replication initiation with cell size regulation in bacteria (Bates & Kleckner, 2005; Boye et al., 1996; Churchward et al., 1981; Hill et al., 2012; Koppes et al., 1980; F. Si et al., 2017; Wold et al., 1994; Zheng et al., 2020; Zheng et al., 2016). An emerging insight is that the regulation of bacterial cell size is not controlled by a single trigger, but rather by a complex and multifactorial process (Jun et al., 2018).

As the regulator of chromosome replication initiation, DnaA plays an essential role in maintaining genome integrity and in ensuring the survival of the bacterial cell. DnaA bound to ATP oligomerizes at the origin of replication (*oriC*), opens *oriC*, and recruits the replication machinery to initiate chromosome replication (Hansen & Atlung, 2018; Kohiyama, 2020). Besides its role in chromosome replication, DnaA also serves as a conserved transcription factor (Menikpurage et

al., 2021; W. Messer & C. Weigel, 1997), albeit fewer mechanistic details are known about this function. DnaA is composed of four structural and functional domains (domains I – IV). The N-terminal domain (domain I) is involved in protein-protein interactions, and it is connected to the AAA+ ATPase domain (domain III) by a helical linker domain (domain II) (Duderstadt & Berger, 2013; Fujikawa et al., 2003). The DNA-binding domain (domain IV) can bind either at *oriC* and initiate chromosome replication or bind at promoter regions and regulate transcription (Hansen et al., 1982). The ability to bind/hydrolyze ATP is essential for DnaA's activity as a replication initiator (Mizushima et al., 1996; Sekimizu et al., 1987). The nucleotide bound (ATP vs. ADP) also modulates DnaA's activity as a transcription factor (Fernandez-Fernandez et al., 2011; Olliver et al., 2010; Speck et al., 1999).

The diderm oligotrophic bacterium *Caulobacter crescentus* is known as an excellent model to study cell cycle regulation, including cell size regulation (Banerjee et al., 2017; Barrows & Goley, 2023; Campos et al., 2014; Govers & Jacobs-Wagner, 2020; Lambert et al., 2018). Upon cell division, *C. crescentus* produces two genetically identical but morphologically distinct cells: a smaller motile swarmer cell that cannot initiate chromosome replication and a sessile stalk cell that is replication competent (Barrows & Goley, 2023) (Figure 1A). The dimorphic life cycle of *C. crescentus* enables isolation of homogeneous populations of cells at different developmental stages (Ardissone et al., 2014; Evinger & Agabian, 1977; Schrader & Shapiro, 2015; Stove & Stanier, 1962). Recently, swarmer cells and stalk cells were shown to grow at different rates despise sharing identical genomes and environments (S. Glenn et al., 2024; T. W. Ng et al., 2024). *C. crescentus* initiates chromosome replication once per cell cycle regardless of nutrient conditions (Marczynski, 1999), which facilitates the analysis of *oriC* copy number per cell size. The genetic circuit that regulates the forward progression of the cell cycle has been extensively characterized in *C. crescentus* revealing that each transcription factor in the circuit regulates each other's expression leading to oscillating abundance of global regulators (J. Collier et al., 2006; Kirkpatrick & Viollier, 2012). DnaA is one of the master transcription factors that make up this genetic circuit (Justine Collier et al., 2006; A. K. Hottes et al., 2005).

In this study, we identify and characterize a new mechanism of DnaA's regulation of cell size that is independent of *oriC*-copy number. We found that increasing the cellular levels of DnaA 3-fold (referred here as 3x-DnaA cells) results in a reduction of cell size by ~20% without impacting chromosome replication. This effect of DnaA on cell size is independent of parameters previously implicated with cell size regulation, like protein synthesis and the alarmone ppGpp molecule. Our transcriptional and mutant analyses revealed that DnaA's activity as a transcription factor is involved in the regulation of cell size. 3x-DnaA cells display increased expression of genes involved in cell wall biosynthesis, including the conserved *murD* and *mraY*. The increased expression *murD* alone results in cells displaying a reduced cell size irrespective of media type (rich and minimal). We discovered that this connection between *murD* and reduction in cell size is conserved in the evolutionary diverse bacterium *E. coli.* After analyzing multiple cell cycle

parameters, our data revealed that the only parameter that changed in 3x-DnaA small cells compared to WT cells is the rate of cell elongation. In fact, elongation rate slowed down also by ~20% consistent with a similar percent reduction in cell size and consistent with cell wall biosynthesis being involved.

RESULTS

DnaA levels impact cell size independent of oriC copy number

A common strategy to study the essential protein DnaA is to use constructs where the native *dnaA* gene is knockout and a *dnaA* copy is engineered to be expressed from inducible promoters. While characterizing such constructs, we noticed that cells expressing *dnaA* from the inducible promoter vanillate (*dnaA*::Ω, P_{van}-*dnaA*) are smaller compared to wildtype cells with *dnaA* at its native locus (Figure 1B). This DnaA-dependent reduction in cell size was only present when cells were grown in minimal media (M2G) but not in nutrient rich media (PYE). The quantification of cell size revealed that in minimal media cell length decreased ~20 % whereas the width remained the same (Figure 1CD). The observed changes only in length are consistent with previous reports showing that *C. crescentus* regulates its size by modulating the cell length (Campos et al., 2014). To ensure that this effect was not in response to the inducer vanillate, we analyzed the cell size of cells expressing *dnaA* from the other commonly used promoter, P-xylose (Thanbichler et al., 2007). Our data revealed that cells expressing *dnaA* from either inducible promoter displayed the same reduction in cell size when grown in minimal media (Supplemental Figure 1A).

Given that DnaA initiates replication at *oriC* and *oriC* copy number are correlated with cell size (Moselio Schaechter et al., 1958), we examined the possibility that changes in *oriC* copy number caused the change in cell size. In *C. crescentus*, replication initiates only once per cell cycle resulting in cells with one or a maximum of two *oriC* copies (Marczynski, 1999). To quantify *oriC* copy number, we used the centromere-like region *parS* (~8 kilobases away from *oriC*) as proxy of number of origins of replication (Thanbichler & Shapiro, 2006; Toro et al., 2008). We fluorescently labeled the *parS*-binding protein ParB and tracked the number of CFP-ParB foci. Our data showed that cells expressing *dnaA* from inducible promoters (*dnaA*::Ω, *parB::cfp-parB,* $P_{van\ or\ xyl}$-*dnaA*) displayed wildtype numbers of *oriC* copies per cell (Figure 1E), discarding the possibility that changes in *oriC* copy number are responsible for the effect on cell length. Consistent with no alteration in *oriC* copy number, cells expressing *dnaA* from inducible promoters grew at similar doubling rates as wildtype cells in rich or minimal media (Figure 1F)

Taking advantage of *C. crescentus* asymmetric cell cycle, we examined whether the DnaA-dependent impact on cell length was specific to the developmental stage of the cell. We wondered about this possibility based on the recent findings that *C. crescentus* shows differential growth rates through their cell cycle (Skye Glenn et al., 2024; Tin Wai Ng et al., 2024). To test this hypothesis, we analyzed cell size of isolated homogeneous population of swarmer cells (Evinger & Agabian, 1977; Schrader & Shapiro, 2015). Our analysis revealed that swarmer cells and

stalked cells display a similar ~20% reduction in cell length (Figure 1G) demonstrating that the impact on cell size is not specific to the developmental stage of the cell. Collectively, these data revealed that changing *dnaA's* transcriptional regulation result in a reduction of cell length independent of both *oriC* copy number and cell cycle stage.

Cell length decreases as DnaA levels increase

The levels and activity of DnaA as a replication initiator are regulated at a multitude of levels, including post-transcriptionally and post-translationally (Felletti et al., 2019; Katayama et al., 2010). In *C. crescentus*, the DnaA levels are 3- to 4-fold higher when grown in rich media than in minimal media (Justine Collier et al., 2006; Frandi & Collier, 2019; Jared M Schrader et al., 2016). Given that our observed reduction in cell length was linked to *dnaA*'s transcriptional regulation (native vs. inducible promoter), we examined whether the levels of the protein DnaA had changed when expressed from inducible promoters. Using western blot analysis with antibodies specific to DnaA, we found that the small cells (*dnaA*::Ω, *parB::cfp-parB,* $P_{van\ or\ xyl}$*-dnaA*) grown in minimal media display ~3-fold higher levels of DnaA compared to wildtype grown under the same condition (Figure 2A). In rich media, however, we observed no differences in DnaA levels between wildtype and cells expressing *dnaA* from inducible promoters. These data suggested that the levels of DnaA protein, and not necessarily the type of media, were the cause of the change in cell size.

To evaluate our hypothesis that elevated DnaA levels contribute to the observed reduction in cell length, we sought to identify conditions that would increase DnaA levels in cells cultured in nutrient-rich media. To increase the levels of DnaA, we constructed two chromosomal *dnaA* merodiploid strains: one with *dnaA* under its native locus plus a copy under an inducible promoter (P_{van}*-dnaA*) or a strain with two copies of *dnaA* under two different inducible promoters (P_{van}*-dnaA* P_{xyl}*-dnaA*). The quantification of DnaA levels with western blots revealed that none of the chromosomal *dnaA* merodiploid strains grown in rich media produced higher levels of DnaA than wildtype. To achieve higher levels of *dnaA* overexpression, we constructed a *C. crescentus* strain with *dnaA* overexpressed from a replicating plasmid. Considering that this approach can lead to over-initiation of chromosome replication, we induced expression of *dnaA* for only ~2 cell cycles in rich media (3h induction). Using western blots, we confirmed that 3h induction results in ~3-fold higher DnaA levels compared to wildtype (Supplementary Figure 2A). However, even under this short-term induction, we observed a significant percent of cells (>10%) over-initiated chromosome replication (Supplementary Figure 2B). To avoid the implications that over-initiation of chromosome replication has on cell size, we continued our analysis using only chromosomal inducible promoters and only minimal media as the growth condition. Later in this manuscript, we revisit rich media as a variable of cell size.

Having determined the upper limits of DnaA levels in minimal media that maintain the normal 1-2 *oriC* copies per cell, we next examined whether the changes in cell length are proportional with the cellular levels of DnaA. We used western blot analysis to first confirm that increasing levels of

inducer correlated with increasing levels of DnaA (Figure 2B). Notably, as the levels of DnaA increased, we observed a corresponding decrease in cell length (Figure 2C). We were able to reach the highest expression levels of DnaA (without over-initiation of replication) when cells were grown with the inducer xylose as the sole carbon source (no glucose added since glucose can inhibit the xylose promoter (Stephens et al., 2007)). Consistent with our hypothesis, our analysis showed that the highest DnaA concentration also results in the highest decrease in cell length in cells grown in minimal media (Figure 2D). Collectively, these data demonstrate that increases in DnaA levels, without impacting replication initiation, linearly correlate with decreases in cell length.

Rate of lateral cell growth is slower in small cells compared to wildtype

We next determined how cells expressing 3x-DnaA levels became smaller. For simplicity, we will refer to cells expressing *dnaA* from an inducible promoter grown in minimal media as 3x-DnaA cells. *C. crescentus*, like most rod-shaped bacteria, undergo different growth phases over the cell cycle: pure elongation phase where new PG is inserted along the lateral walls followed by the zonal phase, where new PG is added at the division site (Aaron et al., 2007). Thus, we hypothesized that 3x-DnaA cells' reduction in size was due to slower cell growth, faster constriction rate, or a combination of both scenarios. To test this hypothesis, we imaged synchronized 3x-DnaA cells (*dnaA*::Ω, *parB::cfp-parB, P_{van}-dnaA*) and wildtype cells over time through one complete cell cycle starting from the G1 phase (swarmer state) through the completion of cytokinesis. Each individual cell was then analyzed through the progression of its cell cycle using an automated analysis with the Fiji plugin MicrobeJ (Ducret et al., 2016; Schindelin, Arganda-Carreras, Frise, Kaynig, Longair, Pietzsch, Preibisch, Rueden, Saalfeld, Schmid, et al., 2012). We calculated for each cell the rates of cell growth and the rates of constriction (Mahone et al., 2024). Our data revealed that the constriction rate remained the same in 3x-DnaA small cells compared to wildtype cells (Figure 3AB). Unlike constriction rate, we discovered that 3x-DnaA small cells elongate at a rate ~20% slower than wild-type cells (Figure 3AC). These exciting results correspond to the observed ~20% reduction in cell length in 3x-DnaA cells.

Cell size determinants and their connection to DnaA.

Numerous factors have been reported to positively influence bacterial cell size, although the precise molecular mechanisms underlying these regulations has remained elusive. We investigated whether the observed DnaA-dependent effect on cell length is connected to previously reported determinants of cell size in bacteria. For instance, reducing the total protein content in the cell has been shown to correlate with a reduction in cell size (Basan et al., 2015). In *B. subtilis,* reducing the synthesis of proteins (using subinhibitory levels of the ribosome targeting antibiotic chloramphenicol) results in ~10% cell length reduction without changes in cell

width (Vadia et al., 2017). Analogous to *B. subtilis*, our analysis of wildtype *C. crescentus* cells exposed to sub-lethal concentrations of chloramphenicol revealed a reduction in cell length by approximately 10%, while cell width remained unchanged (Figure 3D). Notably, the already small 3x-DnaA cells became even smaller by approximately 10% when exposed to chloramphenicol compared to the no antibiotic condition (Figure 3D). These results revealed that DnaA's effect on cell size is independent from the effect that protein content has on cell size regulation. The influence of chloramphenicol on the curvature of *C. crescentus* (Cabeen et al., 2009) remained unchanged in 3x-DnaA cells compared to wildtype (Supplemental Figure 3A).

The alarmone molecule guanosine tetra- or pentaphosphate (p)ppGpp, a global inhibitor of biosynthesis, has been implicated in cell size in various bacterial species. The cellular levels of (p)ppGpp are regulated by the Rsh family enzymes RelA & SpoT (Srivatsan & Wang, 2008; Tozawa & Nomura, 2011). Unlike *E. coli* and *B. subtilis*, *C. crescentus* and other alphaproteobacterial species only encode the SpoT-dependent pathway (Wells & Long, 2002) In *E. coli*, levels of (p)ppGpp have been shown to impact cell size upon amino acid starvation (Traxler et al., 2008). In *C. crescentus*, artificially increasing the levels of (p)ppGpp by expressing a constitutively active RelA from *E. coli* results in cells with decreased cell size (Gonzalez & Collier, 2014). To examine whether DnaA's impact on cell length was connected to levels of (p)ppGpp, we constructed a mutant strain unable to synthesize (p)ppGpp by knocking out the gene encoding the bifunctional (p)ppGpp synthetase/hydrolase SpoT. Our analysis revealed that wildtype cells with and without *spoT* retained the same cell size (Figure 3E). Similar to wildtype cells, 3x-DnaA cells with or without *spoT* display the same cell size demonstrating that the alarmone molecule (p)ppGpp is not connected to the observed DnaA-dependent change in size.

The biosynthesis of fatty acid and cell wall have also been implicated with cell size regulation. To examine whether fatty acid and peptidoglycan (PG) biosynthesis were linked to the reduction in size of 3x-DnaA cells, we followed established protocols to obstruct their biosynthesis using sub-lethal concentrations of the antibiotics cerulenin and Fosfomycin. Cerulenin inhibits the first condensation reaction between acetyl-CoA and malonyl-acyl-carrier-protein catalyzed by FabH (b-ketoacyl-acyl-carrier protein synthase) (Cronan, 2014). In *B. subtilis* and *E. coli*, exposure to cerulenin result in ~10% reduction in cell length (Fangwei Si et al., 2017; Vadia et al., 2017). Unfortunately, we are unable to make any conclusions about cerulenin because we found that the viability of *C. crescentus* is highly sensitive to even low levels of cerulenin (Supplemental Figure 3B). One potential explanation to this high sensitivity is that *C. crescentus* encodes a single copy of FabH whereas *B. subtilis* has two FabH homologs FabHA and FabHB (Kaneda, 1991; Yao et al., 2012). Regarding PG biosynthesis, Fosfomycin is used to inhibit the first committed enzyme, MurA (UDP-N-acetylglucosamine enolpyruvyl transferase) (Typas et al., 2012). Fosfomycin exposure in wildtype *C. crescentus* cells has been reported to cause cells to increase length and width (Harris & Theriot, 2016; Irnov et al., 2017). When we analyzed wildtype cells exposed to similar levels of Fosfomycin (5 μg/mL), we found that indeed cells become bigger in length and width (Supplemental Figure 3C). However, our analysis of *oriC* copy number in both wildtype and

3x-DnaA cells exposed to Fosfomycin revealed that these larger cells over-initiate chromosome replication resulting in abnormal >2 *oriC* copies per cell (Supplemental Figure 3D). Because we cannot resolve whether multiple *oriC* copies caused the cell size increase or cell size increase caused the over-initiation of chromosome replication, we cannot make any conclusions based on these data about the potential connection between DnaA and PG biosynthesis. Based on these analyses of known determinants of cell size regulation in bacteria, our data revealed that protein synthesis and (p)ppGpp are not connected to the reduction in size of 3x-DnaA cells. We will revisit PG biosynthesis later in this manuscript.

DnaA requires binding to both ATP & DNA to exert impact on cell length

To gain insights into the mechanism of how DnaA influences cell size, we examined the role of the various domains of this master regulator (Figure 4A) by constructing a set of variants that included truncations or amino acid modifications targeting these domains. Because DnaA is essential and minor modification to any of these domains can impact viability, we analyzed the effects on cell size using merodiploid strains. These merodiploid strains express variants of DnaA from an inducible chromosomal promoter (P_{xyl}) while the native copy of *dnaA* remains intact. Our data revealed that this type of constructs with wildtype *dnaA* expressed from *Pxyl* (P_{xyl}-*dnaA*) also display the ~20% reduction in cell length when DnaA levels are increased ~3-fold (Figure 4C, Supplemental Figure 4A). We confirmed that the expression of DnaA variants from P_{xyl} had no dominant negative effect on viability using colony forming units (CFU) (Figure 4B). Presence of protein variants compared to empty vector control (EV) was confirmed with western blots (Figure 4C).

In *C. crescentus*, an alanine-rich region at the N-terminal end of domain I is involved in the regulation of cellular levels of DnaA upon nutrient starvation (Felletti et al., 2021). We reasoned that if this ala-rich domain was involved in triggering the change in cell size, increasing the levels of a truncated version of DnaA missing this alanine rich region would have no effect on cell length. However, cells expressing a truncation of the alanine rich region expressed from P_{xyl} (referred as Δala) retained their ability to reduce their cell length (Figure 4D), albeit to marginally lower levels. The small difference in cell length reduction (~18% vs. ~22%) can be attributed to lower levels of expression of this variant compared to cells with 3x-wildtype-DnaA (Figure 4C). These data further support that the impact on cell length is dependent on DnaA levels, and that the alanine rich N-terminal domain is not responsible in DnaA's regulation of cell length.

We considered another possibility were DnaA's role with cell size regulation was independent of its ability to bind DNA. We posit that DnaA itself could regulate cell size potentially by directly modulating the activity of cell size regulators independent of DNA binding. We tested this hypothesis by analyzing the effect on cell length from a DnaA variant with the DNA-binding domain (domain IV) truncated (referred as ΔIV). Expression of this DNA-binding variant had no effect on cell length compared to wildtype levels of DnaA (Figure 4D), revealing that DnaA's ability to bind

DNA is required for its role with cell size regulation. Wondering whether ATP binding and/or hydrolysis was required for DnaA's impact on cell length, we analyzed a variant with a single amino acid substitution that interrupts ATP binding. We did not analyze DnaA variants unable to hydrolyze ATP because such variants are stuck in the active form and over-initiate chromosome replication, which would inevitably impact cell size in an *oriC* copy dependent manner. We constructed DnaA-K195I, a variant encoding a mutation in the Walker A box that affects DnaA's ability to bind ATP (Mizushima et al., 1998). Our data revealed that DnaA-K195I lost the effect on cell length and cells expressing this variant displayed wildtype cell size (Figure 4D).

Collectively, the analyses of DnaA variants revealed that DnaA requires to bind DNA and to bind ATP to cause the effect on cell size. Given that DNA-binding and ATP-binding are involved in regulating both functions of DnaA (chromosome replication initiator and transcription factor), we set out to differentiate DnaA's effect on cell length between these two functions. Because we cannot uncouple these two functions without altering the proper progression of the cell cycle and thus cell size regulation, we proceeded by analyzing each function independently.

Chromosome replication remains unchanged in 3x-DnaA small cells

The initiation of chromosome replication requires DnaA-ATP oligomerization at *oriC*, which opens the double stranded DNA allowing for components of the replisome to assemble and to initiate replication bidirectionally (Leonard & Grimwade, 2011). We explored the possibility that 3x-DnaA levels could alter the overall process of chromosome replication, potentially leading to the reduction in cell size. To test this hypothesis, we used time-lapse microscopy to image synchronized swarmer cells throughout their cell cycle, focusing on three key events of chromosome replication: (a) timing of replisome assembly, (b) timing of replication initiation, and (c) progression of the replication forks (Figure 5). To track replisome assembly, we imaged a strain encoding the replisome component DnaN (β-clamp) fluorescently tagged at *dnaN's* native chromosomal locus (Collier & Shapiro, 2009; Jensen et al., 2001). Our analysis of the time when the DnaN-mCherry focus emerges revealed that the 3x-DnaA small cells and wildtype cells assembled their replisomes at similar times (Figure 5A). To determine timing of replication initiation, we tracked the appearance of two *parS* loci (8kb from *oriC*) using the *parS*-binding protein CFP-ParB (Toro et al., 2008). Our data revealed the 3x-DnaA small cells initiate chromosome replication at similar times as wildtype cells (Figure 5B). Lastly, we examined replisome progression by comparing when a chromosomal locus near the gene *pleC* (1.3 Mb from *oriC*) is replicated. To track replication of *pleC*, we used a strain engineered to encode the Yersinia pestis sequence of *parS(*pMT1) near the *pleC* locus and the corresponding ParB(pMT1) fluorescently labelled expressed from an inducible promoter (Schwartz & Shapiro, 2011). We included to this strain a fluorescent tag with the *C. crescentus'* native ParB as an internal control. Analyzing the timing of replication of *parS* and *pleC* revealed no difference between wildtype and

3x-DnaA small cells (Figure 5C). Overall, these data indicate that the higher levels of DnaA in 3x-DnaA small cells do not alter the overall process of chromosome replication.

Small cells display changes in transcriptional profiles

After demonstrating that 3x-DnaA levels do not affect the progression of chromosome replication, we proceeded to investigate DnaA's other conserved role as a master transcriptional regulator. (Alison K. Hottes et al., 2005; Walter Messer & Christoph Weigel, 1997; Washington et al., 2017). In *C. crescentus*, the DnaA transcriptional regulon includes genes encoding components of the replisome, cell cycle regulators, and nucleotide biosynthesis (A. K. Hottes et al., 2005). We hypothesized that DnaA regulates cell size through its activity as a transcription factor. To test this hypothesis, we examined whether the levels of the transcriptional regulon of DnaA changed in 3x-DnaA small cells. For these analyses, we used the *dnaA* merodiploid strains to enable comparisons with the DnaA variants. When comparing 3x-DnaA (P_{xyl}-*dnaA*^{WT}) with an empty-vector control, our RNA-Seq analysis revealed relatively few genes change expression: 45 total genes with 35 upregulated and 10 downregulated (≥1.5-fold change and FDR<0.05) (Supplemental Table 1). To further exclude non-contributing factors responsible for changes in cell length, we compared RNA-Seq changes between P_{xyl}-*dnaA*^{WT} cells (exhibiting reduced size) and P_{xyl}-*dnaA-K195I* (displaying unaffected cell size). Using this strategy with the same parameters of ≥1.5-fold change and FDR<0.05, our list of potential genes was reduced to 23 (Table 1). From this list we focused on genes involved in cell cycle progression. To validate our hits, we used constructs with chromosomal merodiploid strains to circumvent the high expression levels associated with replicating plasmids, given that the genes of interest exhibited changes of less than 2-fold.

The 1.5-fold increase in expression of the *ftsZ* gene in 3x-DnaA cells (*parB::cfp-parB*, P_{xyl}-*dnaA*^{WT}) cells immediately stood out for multiple reasons (Figure 6A): *ftsZ* is part of the transcriptional regulon of DnaA (Alison K. Hottes et al., 2005); the transcriptional regulation of *ftsZ* is dependent on the nucleotide-bound to DnaA (Fernandez-Fernandez et al., 2011); and FtsZ is a key regulator of the divisome, the molecular machinery that drives cytokinesis and cell wall biosynthesis at the septum (Sackett et al., 1998), both functions that can directly impact cell size. To characterize the potential role of FtsZ, we examined whether the levels of the FtsZ protein were higher in 3x-DnaA cells compared to empty vector, like our transcriptomics data suggested. Using western blots with FtsZ specific antibodies (gift from Erin Goley's Lab), our data revealed no clear differences in FtsZ levels (Figure 6B). To further characterize whether elevated levels of FtsZ lead to a reduction in cell size, we constructed a chromosomal *ftsZ* merodiploid strain (*parB::cfp-parB*, P_{xyl}-*ftsZ*) that displayed increased levels of FtsZ (Supplementary Figure 6A). Our data revealed that increasing FtsZ levels does not decrease cell length. Instead, cells with increased FtsZ levels retain similar size as wildtype but they generate mini-cells (Figure 6C, Supplementary Figure 6B), consistent with previous reports (Goley et al., 2010). These data demonstrate, that FtsZ is not the key player

in the reduction of cell size in 3x-DnaA cells. No changes in FtsZ protein levels in 3x-DnaA cells are consistent with our findings that these small cells display no changes in their constriction rate (Figure 3B).

Another notable gene within DnaA's transcriptional regulon is *gcrA*, which exhibited a 1.8-fold increase in 3x-DnaA cells (Figure 6A). This gene encodes for the master transcription factor GcrA (Justine Collier et al., 2006). GcrA regulates the transcription of ~200 genes, many of which are critical in the progression through the S-phase and later stages of the cell cycle (Haakonsen et al., 2015). To test whether increased levels of GcrA cause cells to reduce their cell length, we constructed a *gcrA* chromosomal merodiploid strain (*parB::cfp-parB, P_{xyl}-gcrA*). Increased expression of the master transcription factor GcrA resulted in cells with longer cell length, instead of shorter (Figure 6C,D), consistent with previous reports (Haakonsen et al., 2015; Holtzendorff et al., 2004).

We next explored an alternative hypothesis where DnaA regulates cell size indirectly through the transcriptional regulon of GcrA. From our list of 23 genes, we focused on three genes that are part of the GcrA regulon and are conserved in bacteria: *dnaG* (+1.8-fold) involved in DNA replication, *murD* (+1.5-fold) and *mraY* (+1.6-fold) involved in PG biosynthesis. The DNA primase DnaG represented an interesting target to regulate cell size because DnaG directly regulates the rate of DNA replication in a ppGpp-dependent manner (Levine et al., 1991; Maciag et al., 2010). To test DnaG's potential role with cell size regulation, we analyzed a *dnaG* chromosomal merodiploid strain (*parB::cfp-parB, P_{xyl}-dnaG*) and found that induction of *dnaG* results in no changes in cell size (Figure 6CD). These results are consistent with our findings that ppGpp and the overall process of DNA replication are not involved in the cell size reduction of 3x-DnaA cells.

Peptidoglycan biosynthesis plays a critical role in the regulation of cell size given that it directly facilitates the expansion of the cell envelope during cell growth and during constriction at the division plane (Aaron et al., 2007). MurD is one of the four cytoplasmic ATP-dependent enzymes that catalyze the successive additions of amino acids to UDP-N-acetylmuramic acid in PG biosynthesis (Typas et al., 2012). MraY transfers UDP-N-acetylmuramic acid-pentapeptide onto the lipid carrier bactoprenol forming the intermediate known as lipid I (Ikeda et al., 1991). To test the hypothesis that changes in MurD and/or MraY levels were responsible for the changes in cell size observed in 3x-DnaA small cells, we constructed chromosomal merodiploid strains of each to titrate the levels of these proteins using wildtype as the parent strain. Induction of *mraY* expression in the merodiploid strain (*parB::cfp-parB, P_{xyl}-mraY*) did not reduce cell length but instead caused a subtle but significant increase in cell length compared to empty vector (Figure 6C,D). Excitingly, analysis of the *murD* merodiploid strain (*parB::cfp-parB, P_{xyl}-murD*) revealed that induced expression of *murD* results in cells with ~10% reduction in cell size (Figure 6D).

MurD as a key player of cell size independent of growth media

Altering the expression of *murD* was the only genetic modification from our RNA-Seq analysis that led to a decrease in cell size. Wondering whether we could achieve an even greater reduction in cell size by further increasing *murD* expression beyond the already higher levels in 3x-DnaA cells, we constructed a *murD* merodiploid strain using the 3x-DnaA cells as the parent strain (*parB::cfp-parB, dnaA*::Ω, P_{van}-*dnaA*, P_{xyl}-*murD*). Our data revealed that indeed, induction of *murD* overexpression in the 3x-DnaA cells results in an additional ~10% decrease in cell length (Figure 7A). However, the higher induction of *murD* in 3x-DnaA cells and/or their smaller cell size led to a defect on growth rate (Figure 7B), demonstrating the importance of maintaining proper levels of MurD. Having identified MurD as a key player in the regulation of cell size, we reconsidered the growth media type and analyzed whether increasing *murD* expression alone results in cell size changes when cells are grown in rich media. Indeed, our data revealed that induction of *murD* in the merodiploid strain with native levels of DnaA grown in rich media displayed a ~10% reduction in cell length compared to empty vector control without impacting growth rate. (Figure 7C,D). These findings support MurD's involvement in cell size regulation that is independent of growth media type.

MurD's impact on cell size is conserved

The gene encoding *murD* is part of the division and cell wall (dcw) gene cluster that is highly conserved across bacteria in both order of genes and content of genes (Megrian et al., 2022; Nikolaichik & Donachie, 2000). Having identified MurD as a key player of cell size, we posit whether MurD's impact on cell size was conserved outside the alpha-proteobacterium *C. crescentus*. To address this question, we used the evolutionarily distant gamma-proteobacterium *Escherichia coli*. We constructed a *murD* merodiploid *E. coli* strain with the second copy of *murD* expressed from the arabinose-inducible low copy expression vector *pBAD* (MG1565 p(*murD*)). *E. coli* cells were induced for 3 h and analyzed at OD_{600nm} between 0.2 – 0.3. Notably, our data revealed that *E. coli* with *murD* overexpression displayed ~10% reduction in cell size compared to the empty vector control (Figure 7E). This change in cell size did not impact the doubling rate of cells (Figure 7F). These data suggest that the role of MurD in modulating cell size is conserved among bacteria.

DISCUSSION

Despite significant advances in our understanding of how environmental and genetic perturbations can impact cell size within a population, details about the molecular mechanisms underlying bacterial cell size regulation have remained elusive. One emerging insight is that the regulation of cell size is governed by a complex and multifactorial process. In this study, we examined the influence of the replication initiator DnaA with cell size independent of *oriC* copy numbers. Our data revealed that DnaA is involved in cell size regulation through DnaA's activity as a transcription factor. By inducing a modest increase (3-fold) in DnaA levels without altering initiation or progression of chromosome replication, our data revealed that cells reduce their elongation rate resulting in cells with smaller cell length. We show that DnaA impacts cell size by indirectly regulating the transcriptional levels of key enzymes involved in cell wall biosynthesis.

DnaA is a global transcriptional regulator in bacteria. DnaA's transcriptional regulon commonly includes other global regulators involved in genome maintenance, cell development, and pathogenesis (Krusenstjerna et al., 2023). In *B. subtilis*, DnaA is connected to the onset of sporulation by transcriptionally regulating an inhibitor of the sporulation master transcription factor SpoOA. In *Borrelia burgdorferi*, DnaA regulates the transcription of the nucleoid associated protein EbfC which itself regulates the transcription of a multitude of other genes (Jutras et al., 2012; Krusenstjerna et al., 2023). Furthermore, altering the transcriptional activity of DnaA in *B. burgdorferi* lead to changes in >20 components of the elongasome and divisome, which could also connect DnaA to cell wall biosynthesis (Krusenstjerna et al., 2024). Our work revealed that in *C. crescentus*, DnaA regulates cell size by modulating cell wall biosynthesis through the activation of its master transcription factor GcrA. These findings highlight the global impact of DnaA and its conserved ability to coordinate cell development in bacteria directly and indirectly.

Another major cell cycle regulator implicated in the regulation of cell size is the tubulin-like FtsZ protein. The activity of FtsZ (GTP-dependent polymerization) is regulated by multiple factors that promote the assembly or disassemble of the polymer. The levels of FtsZ are regulated at the transcriptional level and by ATP-dependent proteolysis (Morrison & Camberg, 2024; Weart & Levin, 2003). In *C. crescentus*, the expression of *ftsZ* and proteolysis of FtsZ are tightly regulated over the cell cycle (Iniesta et al., 2006; Kelly et al., 1998; J. M. Schrader et al., 2016; Williams et al., 2014). The accumulation of threshold levels of FtsZ were shown to be critical for determining cell size in both *E. coli* and *B. subtilis* (Si et al., 2019). An increase in *ftsZ* transcription in our 3x-DnaA small cells initially suggested an earlier onset and/or faster constriction rate that would lead to smaller cells. Despite the 3-fold increase in transcript of *ftsZ*, the 3x-DnaA small cells displayed the same concentrations of FtsZ protein as wildtype cells and thus exhibited no changes during constriction. Unlike FtsZ, our increase in transcription of *dnaA* led to a corresponding increase in the levels of the protein DnaA: ~3-fold increase in *dnaA* transcript led to ~3-fold increase in DnaA

462 protein levels. These findings highlight the distinctions in the multi-tiered regulation of two principal
463 cell cycle regulators, DnaA and FtsZ, both of which influence cell size.

464 Cell wall biosynthesis has been implicated with cell size regulation in bacteria (Cesar &
465 Huang, 2017). *B. subtilis* regulates cell width by balancing the activity of two opposing
466 mechanisms involved in cell wall remodeling: Rod complex and class A penicillin-binding proteins
467 (aPBPs) (Dion et al., 2019). In *C. crescentus*, deregulation of the inhibitor AimB of the cytoskeletal
468 protein MreB (part of the Rod complex) was shown to impact cell shape and cell length (Werner
469 et al., 2020). Our data revealed that small cells with 3-fold higher levels of DnaA upregulate the
470 expression of the transcription factor GcrA and the expression of cell wall biosynthetic enzymes
471 MurD and MraY. GcrA regulates the transcription of the operon where *murD* and *mraY* are found
472 side-by-side. The organization of *murD*, *mraY* and other essential genes involved in cell wall
473 biosynthesis is remarkably conserved in bacterial (Megrian et al., 2022). Increasing the
474 expression of *gcrA* or *mraY* both led to cells with increased cell length. However, increasing the
475 expression of *murD* alone led to a reduction in cell length without altering the growth rate of those
476 cells. These data indicate that DnaA regulates the levels of various factors involved in cell wall
477 biosynthesis and cell cycle progression, which collectively function to control cell size.

478 Bacteria have been known to follow the Growth law, which states that cell size is an
479 exponential function of growth rate (Donachie et al., 1976; Sargent, 1975; M. Schaechter et al.,
480 1958; Weart et al., 2007; Woldringh et al., 1980). We show that MurD's impact on cell size is
481 independent of nutrient availability. Cells with increased *murD* expression in wildtype background
482 reduced their size when grown in minimal or rich media. We discovered that further increase of
483 *murD* expression results in a further reduction in cell size that was interestingly accompanied by
484 a decrease in growth rate. This phenomenon may be attributed to the reduced cellular volume
485 interfering with essential housekeeping processes during the cell cycle or a potential connection
486 between MurD and the Growth Law. Our finding that MurD can also reduce the size in *E. coli* posit
487 MurD as a conserved regulator of cell size. MurD has garnered significant attention in drug
488 development due to its crucial role in cell wall biosynthesis (Azam & Jupudi, 2020; Sink et al.,
489 2013). This interest is likely to further escalate if MurD is found also critical for regulating cell size.
490 Further investigation into MurD's activity and its role in cell size regulation will yield significant
491 insights into the complex mechanisms governing bacterial cell size.

RESOURCE AVAILABILITY

All data are contained within the manuscript.

ACKNOWLEDGEMENTS

We are grateful to Erin Goley and her lab for providing the FtsZ antibodies, specifically to Jordan M. Barrows for his assistance with the rate of elongation and constriction protocol. We thank Anuradha Sharma from the Sanfilippo lab for her help with the R script. We also thank Dr. Alvaro Hernandez and the Roy J. Carver Biotechnology Center for RNA sequencing, as well as to Dr. Jenny Drnevich for her expertise in the statistical analysis of the RNA-seq data. The work reported in this publication was supported by the National Institute of General Medical Sciences of the National Institutes of Health (NIH) under Award Number R01GM133833 and by the National Science Foundation (NSF) Science and Technology Center for Quantitative Cell Biology under Award Number 2243257.

AUTHOR CONTRIBUTIONS

EK and PEM conceived project and wrote manuscript. EK performed all experiments.

DECLARATION OF INTERESTS

The authors declare no completing interests.

FIGURE LEGENDS

Figure 1. DnaA levels impact cell size. A. (Left) Schematic representation of *Caulobacter* dimorphic lifestyle, highlighting swarmer and stalk cell. **B**. Schematic of WT and *dnaA* inducible strain. Representative images of mixed population WT (CB15N *parB*::CFP-*parB*) and inducible *dnaA* (CB15N Δ*vanA parB*::CFP-*parB vanA*::*dnaA dnaA*::Ω-(spec/strp) cells grown in minimal media, scale 2μm. Cells were grown overnight with PYE or M2G to exponential phase with relevant inducer before microscopy. **C.** Super plots showing cell length analysis of mixed population grown in rich media (PYE) and minimal media (M2G). Small dots represent data points from three independent replicates, large dots represents median values (blue, pink, yellow). The horizontal line represents the mean of three median values. *dnaA* inducible shows ~20% decrease in cell size when grown in minimal media. **D.** Super plots showing cell width analysis of mixed population grown in rich media (PYE) and minimal media (M2G). **E**. Percentage cells representing *oriC* quantification in WT and inducible *dnaA* strain **F.** Growth curves (top panel) representing rich media and lower panel representing minimal media. WT is shown as blue dots and *dnaA* inducible as yellow dots. **G.** Super plots showing cell length analysis of synchronized population grown in rich media (PYE) and minimal media (M2G). Data points show mean ± SD. A parametric t test was performed using population mean values (N = 3) to compare values for each measurement. p(<0.0001) ****, p(0.0001)***, p(<0.05)*, ns (non-significant). n= ~600 cells

Figure 2. Changing DnaA levels corelates to cell size. Cells were grown overnight in M2G or PYE to exponential phase with inducer before sample preparation and microscopy. **A.** Western blot showing DnaA levels of WT and inducible *dnaA* (CB15N Δ*vanA parB*::CFP-*parB* vanA::*dnaA dnaA*::Ω-(spec/strp) cells grown in rich and minimal media. Quantification of western blot showing significant differences in *dnaA* inducible vs WT grown in minimal media. Inducible *dnaA* strain shows 3-fold more DnaA in comparison to WT. **B.** Western Blot showing DnaA titration using WT and inducible *dnaA* (CB15N Δ*vanA parB*::CFP-*parB xylX*::*dnaA dnaA*::Ω-(spec/strp). Levels of DnaA were titrated using inducible *dnaA* strain using xylose as inducer. Xylose was titrated from 0.025%, 0.05%, 0.075% to 0.3% in M2G, cells grown in M2X are shown after the dotted line. **C.** Quantification of DnaA levels show as the inducer percentage increases, DnaA levels are increased in the inducible strain in comparison to WT in minimal media. **D.** Super plots showing cell length analysis of mixed population grown in minimal media. WT (CB15N *parB*::CFP-*parB*) and titration of inducer with inducible *dnaA* (CB15N Δ*vanA parB*::CFP-*parB xylX*::*dnaA dnaA*::Ω-(spec/strp) strain. Small dots represent data points from three independent replicates, large dots represent median values (blue,grey,orange). At 0.025% xylose the cell size reverts to WT. As the concentration of inducer is increased to 0.050, 0.075, 0.03% in minimal media M2G the cell size decreases gradually, whereas M2X shows further decrease in cell length ~20%. **E.** Quantification of cell length in comparison to WT, the maximum drop is observed with M2X. Data points show mean ± SD. A parametric t test was performed using population mean values (N = 3). p(<0.0001) ****, p(0.0001)***, p(<0.05)*, ns (non-significant). n= ~600 cells

Figure 3. Impact of DnaA on cell size determinants. To test rate of elongation and contriction cells were grown in minimal media overnight with inducer 100μM van to exponential phase before synchrony, timelapse images were taken after very 15minutes. **A.** Representative time-lapse images of WT (CB15N *parB*::CFP-*parB*) and 3x-DnaA (CB15N Δ*vanA parB*::CFP-*parB vanA*::*dnaA dnaA*::Ω-(spec/strp) one cell cycle in minimal media, scale 2μm. Both WT and 3x-DnaA constricts at the same time ~105-120 minutes. **B.** Quantification of rate of constriction remains unchanged between WT and 3x-DnaA. **C.** Quantification of rate of elongation shows it is reduced by ~20% in 3x-DnaA cells. Data points show mean ± SD. A parametric t test was performed using population mean values (N = 3). n=~300 cells. **D.** Impact of protein synthesis inhibition on cell size. *Caulobacter* cells were grown in minimal media overnight with sub-lethal concentration of Chloramphenicol and inducer 100μM van. Super plots showing cell length analysis of mixed population. Small dots represent data points from three independent replicates, large dots represent median values (blue,pink,yellow). WT (CB15N *parB*::CFP-*parB)* cells show a reduction in cell length by approximately 10%, while cell width remained unchanged. 3x-DnaA (CB15N Δ*vanA parB*::CFP-*parB vanA*::*dnaA dnaA*::Ω-(spec/strp) cells show a further approximately 10 % reduction when exposed to chloramphenicol. **E.** Impact of ppGpp on cell size. Super plots showing cell length analysis of mixed population grown in minimal media. WT delta *spoT (*CB15N *parB*::CFP-*parB* Δ*spoT* Δ*vanA)* in comparison to 3x-DnaA delta *spoT* (CB15N Δ*vanA parB*::CFP-*parB vanA*::*dnaA dnaA*::Ω-(spec/strp Δ*spoT*). Cell length analysis shows non-

significant changes between 3x-DnaA and 3x-DnaA delta *spoT*, shows similar decrease in cell length ~20%. Data points show mean ± SD. A parametric t test was performed using population mean values (N = 3). p(<0.0001) ****, p(0.0001)***, p(<0.05)*, ns (non-significant). n= ~600 cells.

Figure 4. DnaA's ability to bind to ATP and DNA is required to cell size regulation

A. AlphaFold model of DnaA, domains color coded in blue- domain I, grey- domain II, yellow- domain III, red- domain IV. DnaA truncations show WT and mutant DnaA. Schematic shows WT and 3x-DnaA (merodiploid WT *dnaA* under P_{xyl}) (CB15N *parB*::CFP-*parB, P_{xyl}-dnaA)*. Cells were grown overnight in minimal media M2G or M2X (xylose as inducer) to exponential phase before serial dilution**,** western sample preparation and microscopy. **B.** Colony forming units showing viability of DnaA mutants in comparison to empty vector EV (CB15N *parB*::CFP-*parB* pXCHYC-2). EV and DnaA mutants show similar growth. **C.** Western blot showing levels of DnaA mutants in comparison to EV and 3x-DnaA. Truncation of domain IV yields 38kDa DnaA. **D.** Superplots showing cell length quantification of EV and DnaA mutants. Small dots represent data points from three independent replicates, large dots represent median values. 3x-DnaA shows ~20% decrease in cell length. Δ*ala* rich region from N-terminus (CB15N *parB*::CFP-*parB P_{xyl}*-Δ*ala* N-ter *dnaA*) shows ~15% decrease in cell length. DnaA ATP*K195I (CB15N *parB*::CFP-*parB P_{xyl}-dnaA ^{K195I})* and DnaA domain IV truncation (CB15N *parB*::CFP-*parB P_{xyl}-dnaA ^{I,II,III}*) reverts back to WT cell length ~2.36μm. Data points show mean ± SD. A parametric t test was performed using population mean values (N = 3). p(<0.0001) ****, p(0.0001)***, p(<0.05)*, ns (non-significant). n=~600 cells

Figure 5. Replication progression remains unchanged in small cells. Cells were grown in minimal media M2G or M2X (xylose as inducer) with 100μM van overnight to exponential phase before synchrony. Timelapse images were taken after very 5minutes for DnaN, and every 15min for *parS* and PleC. **A.** Assembly of replisome using fluorescently tagged DnaN in WT (CB15N *parB*::CFP-*parB dnaN*::*dnaN* mcherry) and 3x-DnaA (CB15N Δ*vanA parB*::CFP-*parB vanA*::*dnaA dnaA*::Ω-(spec/strp) *dnaN*::*dnaN* mcherry). In both strains replisome assembles at ~5min represented with red dot. **B.** Timing of replication initiation was quantified using labelled ParB in WT (CB15N *parB*::CFP-*parB*) and 3x-DnaA (CB15N Δ*vanA parB*::CFP-*parB vanA*::*dnaA dnaA*::Ω-(spec/strp). In both strains, replication initiation happens at ~15-20min, represented with green dot. **C.** Progression of replication using *parS*(pMT1) near the *pleC* locus in WT (CB15N CFP-*parB PvanA*-mCherry-*parB*(pMT1) *parS*(pMT1)-*pleC* (MS513) and 3x-DnaA (CB15N CFP-*parB PvanA*-mCherry-*parB*(pMT1) *parS*(pMT1)-*Pxyl-dnaA*). In both strains we see a second PleC tag appears around ~75min, represented as red dot. Data is representation of three independent experiments. Data points show mean ± SD. A parametric t test was performed using population mean. p(<0.0001) ****, p(0.0001)***, p(<0.05)*, ns (non-significant). n=~100 cells.

Figure 6. DnaA regulates cell size as a transcription factor. Cells were grown in minimal media M2G or M2X (xylose as inducer) overnight to exponential phase before RNA extraction, sample preparation and microscopy. **A.** RNA-seq data represented as volcano plot (left panel) comparing EV (CB15N *parB*::CFP-*parB* pXCHYC-2 to 3x-DnaA (CB15N *parB*::CFP-*parB* P_{xyl}-*dnaA*) represented with dark grey shows 48 genes upregulated and 10 genes downregulated FDR <0.05. Comparison of 3x-DnaA to DnaA K195I (CB15N *parB*::CFP-*parB* P_{xyl}-*dnaA* ^{K195I} is represented with blue dots. **B.** FtsZ levels in WT and 3x-DnaA strain shows comparable levels, FtsZ ~65kDa. **C.** Cell images of EV and merodiploid *ftsZ*, *gcrA*, *dnaG*, *mraY* and *murD,* scale 2µm. Super plots showing cell length quantification of EV (CB15N *parB*::CFP-*parB* pXCHYC-2) and merodiploid (CB15N *parB*::CFP-*parB* P_{xyl}-*ftsZ),* (CB15N *parB*::CFP-*parB* P_{xyl}-*gcrA),* (CB15N *parB*::CFP-*parB* P_{xyl}-*dnaG),* (CB15N *parB*::CFP-*parB* P_{xyl}-*mraY),* (CB15N *parB*::CFP-*parB* P_{xyl}-*murD).* Small dots represent data points from three independent replicates, large dots represent median values
Induction of *murD* shows 10% decrease in cell length in comparison to EV in minimal media.

Figure 7. MurD's impact on cell size. *Caulobacter* cells were grown in minimal media M2G or M2X (xylose as inducer) with 100µM van overnight to exponential phase before microscopy. **A.** Super plots showing cell length quantification of *murD* overexpression. Small dots represent data points from three independent replicates, large dots represent median values. *murD* overexpression in 3x-DnaA background (CB15N Δ*vanA parB*::CFP-*parB vanA*::*dnaA dnaA*::Ω-(spec/strp, P_{xyl}-*murD*) results in an additional ~10% decrease in cell length in comparison to 3x-DnaA (CB15N Δ*vanA parB*::CFP-*parB vanA*::*dnaA dnaA*::Ω-(spec/strp).
B. Growth curves showing induction of *murD* in 3x-DnaA cells leads to a defect on growth rate.
C. Super plots showing cell length quantification *murD* merodiploid (CB15N *parB*::CFP-*parB* P_{xyl}-*murD)* in rich media (PYE) or (PYEX) xylose 0.2% was used to induce expression. *murD* overexpression in rich media shows a similar 10% decrease in cell length. N=~600 cells **D.** Growth curves showing the doubling time remains same when *murD* is overexpressed.
E. coli cells were grown overnight in LB and then back diluted in fresh media with 2% arabinose to induce the expression for 3hrs. Cultures in early exponential phase were used for microscopy and growth curves. **E.** *E. coli* cells grown in rich media. EV (MG1655-pBad) is shown in comparison to *murD* overexpression (MG1565 pBad-*murD*) in rich media with and without inducer arabinose 2%. Cell length decreases by ~10% when *murD* is expressed in comparison to EV with inducer. **F.** Growth curves show that there is no growth defect when *murD* is overexpressed in comparison to EV with and without inducer. Data points show mean ± SD. A parametric t test was performed using population mean values (N = 3). p(<0.0001) ****, p(0.0001)***, p(<0.05)*, ns (non-significant).
N=~250 cells

MATERIALS AND METHODS

Bacterial strains and growth conditions

Plasmids, strains, and primer descriptions are listed in the Supplementary Table S2. *Caulobacter crescentus* strains used in this study were derived from NA1000 (wildtype). Plasmids were constructed by cloning PCR products into pNPTS138,pXCHYC-2, pXMCS-2, pBXMCS-2, pBad vectors (Thanbichler et al., 2007). Amplified PCR products were placed in vectors via Gibson or restriction cloning. Plasmids were transformed into DH5α cells and verified through sequencing. In *C. crescentus*, plasmids were transformed via electroporation. *Caulobacter* strains were grown in peptone yeast extract (PYE) or M2 minimal media supplemented with 0.2% glucose (M2G) or 0.2% xylose (M2X). Liquid cultures were re-inoculated overnight in fresh media to grow cells until exponential phase OD_{600} ~ 0.3-0.4 at 30°C under mechanical agitation 200 rpm. Overnight cultures were supplemented with specific antibiotics and inducers. Vanillate 100μM was used to induce the expression of P_{van}, while 0.3% xylose or M2X was used to induce P_{xyl}. Liquid cultures were supplemented with following concentrations of antibiotics: 5µg/ml kanamycin, 25µg/ml spectinomycin, 5µg/ml streptomycin. For PYE plates 25µg/ml kanamycin, 100µg/ml spectinomycin and 5µg/ml streptomycin. To check the impact of chloramphenicol, cerulenin and fosfomycin, 1/10 sub-lethal concentration of chloramphenicol, 0.6µg/ml cerulenin and 5µg/ml fosfomycin was added to liquid culture and left overnight such that the OD is 0.3 next day.

E. coli strains were inoculated from freezer stock grown in LB at 37°C, liquid culture was supplemented with 50µg/ml ampicillin. Cultures were back diluted with antibiotic and inducer arabinose 2% until exponential phase OD_{600} ~ 0.2-0.3.

Synchronization

C.crescentus cells were synchronized using mini-synchrony protocol to isolate swarmer population (Tsai & Alley, 2001). Cells were inoculated in 15ml M2G overnight, to an OD_{600} ~ 0.3. Cultures were supplemented with inducer and antibiotics as noted. Cells were pelleted at 6000 rpm for 10 minutes at 4°C in centrifuge. Cell pellet was resuspended in 800µl of 1X M2 salts and 900µl of Percoll (Sigma-Aldrich) for density gradient. The mixed solution was centrifuged at 11.000rpm for 20minutes, the bottom layer of swarmer cells was isolated and transferred to a fresh tube. Cells were washed twice with ice cold 1X M2 salts, centrifuged at 8000 rpm for 3 minutes at 4°C. Swarmer's were resuspended in M2G to appropriate OD_{600} ~0.2-0.3.

Growth assays

C.cresentus overnight cultures were grown from freezer stock in M2G or PYE liquid medium were back diluted to reach OD_{600} ~0.1 for growth curves. Early log phase cultures were used for inoculation in 96-well plate in M2G or PYE with relevant inducer. Optical density at 600 nm was monitored every hour at 30°C in a Biotek EPOCH-2 microplate reader with shaking. For *E. coli*, cultures were inoculated from freezer stock and back diluted such that the cells reach early log

phase OD_{600} ~0.1 to inoculate in LB in 96-well plate. Optical density at 600 nm was monitored every 10 minutes at 37°C in a Biotek EPOCH-2 microplate reader with shaking.

Microscopy

Cells were grown to an exponential OD_{600} ~0.3. Cells (1µl) were spotted on agar pads (1% agarose in M2G or M2salts). For time-lapses (2µl) cells were spotted on agar pads.
Phase contrast and fluorescent images were taken at room temperature using Zeiss Axio Observer 2.1 inverted microscope with AxioCam 506 mono camera (objective: Plan-apochromat 100x/1.40 Oil Ph3 M27 [WD=0.17mm]) and Zen Pro software. Samples were blinded for data analysis. To count number of foci, ImageJ (cell counter plugin) was used (Schindelin, Arganda-Carreras, Frise, Kaynig, Longair, Pietzsch, Preibisch, Rueden, Saalfeld, & Schmid, 2012). Cell size (length and width) was analyzed using ImageJ/FIJI plugin MicrobeJ (Ducret et al., 2016). Multiple frames were analyzed for cell size analysis, data were presented in Superplots (Lord et al., 2020).

Elongation and constriction

Cells were grown in liquid cultures with inducer overnight to reach early log phase OD_{600} ~0.3 to synchronize. After synchrony cell were resuspended in M2G or M2X with appropriate additives. Cells were then spotted on agar pads (0.1% agar with inducer) for timelapse. Images were taken after every 15 minutes through one cell cycle. MicrobeJ was used to analyze timelapse images as described by (Lariviere et al., 2018; Mahone et al., 2024). Constriction is automatically detected at the positive curvature midcell and manually segmented upon division. Cell width was detected at the site of constriction whereas cell length was calculated at each time point. Cell width was detected at the site of constriction whereas cell length was calculated at each time point. Constriction time was determined by multiplying the number of frames from constriction initiation to division by 15 (images were taken every 15min). The constriction rate was calculated by dividing the cell width at the onset of constriction by the constriction time. Elongation rate calculated by dividing change in length from constriction initiation to division by constriction time.

Immunoblotting

Caulobacter mixed population cells were grown to early exponential phase OD_{600} ~0.3 with inducer. The OD_{600} of the incubated cultures was normalized to 0.2. Cells were pelted and resuspended in 40µl of cracking buffer, then boiled for 10 min at 90°C. Samples were stored at -20°C for western blotting. A 12% SDS-PAGE gel was used to separate proteins and then transferred to PVD membrane using iBlot2 (Invitrogen Dry Blotting System). The membrane was blocked with 1XTBS (10mM Tris-HCL, pH8,150mM NaCl, 0.1% Tween-20), 0.1% tween 20 (TBST) and 5% non-fat milk at room temperature. The blot was incubated overnight with primary antibody for DnaA (α-DnaA) (Mera et al., 2014) at a dilution of 1:15,000 for FtsZ (α-FtsZ)(Sundararajan et al., 2015) at a 1:20,000 dilution in TBST with 5% milk overnight at 4°C. Next day the membrane was washed 3X with TBST and then incubated with secondary antibody

(α-Rabbit IgG peroxidase, Sigma-Aldrich) diluted to 1:15,000 in TBST with 5% milk at room temperature for 1 hour. The blot was washed 3X with TBST for 5 minutes. To develop the blot, SuperSignal West Pico PLUS Chemiluminescent Substrate (Themo Fisher Scientific) was used and imaged by using ChemiDoc-MP (Bio-Rad). WT DnaA runs at 56kDa, whereas WT FtsZ is 54.1kDa, but it runs at ~65kDa.

CFUs for viability assay

Caulobacter cells were grown from freezer stocks in minimal media M2G or M2X, it was then reinoculated in fresh media with relevant additives at 30°C 180rpm to reach exponential growth OD_{600} ~0.3. Cells were then normalized to OD_{600} ~0.1. Cultures were serially diluted in a 96-well plate and plated on M2G or M2X plates (0.2% xylose in M2X plates was used as inducer). Plates were incubated at 30°C for 2 days and then imaged using ChemiDoc-MP (Bio-Rad).

RNA-sequencing

Caulobacter cells were grown from freezer stocks in minimal media M2G, reinoculated in fresh media M2G or M2X (M2X media to induce the expression of mutants) at 30°C 180rpm to reach exponential growth OD_{600} ~0.3. Total RNA was extracted using hot phenol procedure (Aiba et al., 1981). After total RNA extraction it was treated with DNase (Invitrogen TURBO DNase) to remove genomic DNA and quantitated using nanodrop (Themo Fisher Scientific NanoDrop One^{c}). Samples were then sent to Roy J. Carver Biotechnology Center Sequencing core at UIUC to check RNA integrity through Bioanalyzer, library preparation, sequencing, and data analysis.

REFERENCES

1. Aaron, M., Charbon, G., Lam, H., Schwarz, H., Vollmer, W., & Jacobs-Wagner, C. (2007). The tubulin homologue FtsZ contributes to cell elongation by guiding cell wall precursor synthesis in Caulobacter crescentus. *Molecular Microbiology, 64*(4), 938-952. https://doi.org/https://doi.org/10.1111/j.1365-2958.2007.05720.x

2. Aiba, H., Adhya, S., & de Crombrugghe, B. (1981). Evidence for two functional gal promoters in intact Escherichia coli cells. *Journal of Biological Chemistry, 256*(22), 11905-11910.

3. Amir, A. (2014, 05/23/). Cell Size Regulation in Bacteria. *Physical Review Letters, 112*(20), 208102. https://doi.org/10.1103/PhysRevLett.112.208102

4. Ardissone, S., Fumeaux, C., Berge, M., Beaussart, A., Theraulaz, L., Radhakrishnan, S. K., Dufrene, Y. F., & Viollier, P. H. (2014, Nov 25). Cell cycle constraints on capsulation and bacteriophage susceptibility. *Elife, 3*. https://doi.org/10.7554/eLife.03587

5. Azam, M. A., & Jupudi, S. (2020, 2020/06/01). MurD inhibitors as antibacterial agents: a review. *Chemical Papers, 74*(6), 1697-1708. https://doi.org/10.1007/s11696-020-01057-w

6. Banerjee, S., Lo, K., Daddysman, M. K., Selewa, A., Kuntz, T., Dinner, A. R., & Scherer, N. F. (2017, Jul 24). Biphasic growth dynamics control cell division in Caulobacter crescentus. *Nat Microbiol, 2*, 17116. https://doi.org/10.1038/nmicrobiol.2017.116

7. Barrows, J. M., & Goley, E. D. (2023, Feb 22). Synchronized Swarmers and Sticky Stalks: Caulobacter crescentus as a Model for Bacterial Cell Biology. *J Bacteriol, 205*(2), e0038422. https://doi.org/10.1128/jb.00384-22

8. Bartlett, T. M., Bratton, B. P., Duvshani, A., Miguel, A., Sheng, Y., Martin, N. R., Nguyen, J. P., Persat, A., Desmarais, S. M., VanNieuwenhze, M. S., Huang, K. C., Zhu, J., Shaevitz, J. W., & Gitai, Z. (2017, Jan 12). A Periplasmic Polymer Curves Vibrio cholerae and Promotes Pathogenesis. *Cell, 168*(1-2), 172-185 e115. https://doi.org/10.1016/j.cell.2016.12.019

9. Basan, M., Zhu, M., Dai, X., Warren, M., Sevin, D., Wang, Y. P., & Hwa, T. (2015, Oct 30). Inflating bacterial cells by increased protein synthesis. *Mol Syst Biol, 11*(10), 836. https://doi.org/10.15252/msb.20156178

10. Bates, D., & Kleckner, N. (2005, Jun 17). Chromosome and replisome dynamics in E. coli: loss of sister cohesion triggers global chromosome movement and mediates chromosome segregation. *Cell, 121*(6), 899-911. https://doi.org/10.1016/j.cell.2005.04.013

11. Beveridge, T. (1988). The bacterial surface: general considerations towards design and function. *Canadian Journal of Microbiology, 34*(4), 363-372.

12. Boye, E., Stokke, T., Kleckner, N., & Skarstad, K. (1996, Oct 29). Coordinating DNA replication initiation with cell growth: differential roles for DnaA and SeqA proteins. *Proc Natl Acad Sci U S A, 93*(22), 12206-12211. https://doi.org/10.1073/pnas.93.22.12206

13. Cabeen, M. T., Charbon, G., Vollmer, W., Born, P., Ausmees, N., Weibel, D. B., & Jacobs-Wagner, C. (2009, May 6). Bacterial cell curvature through mechanical control of cell growth. *Embo j, 28*(9), 1208-1219. https://doi.org/10.1038/emboj.2009.61

14. Campos, M., Surovtsev, I. V., Kato, S., Paintdakhi, A., Beltran, B., Ebmeier, S. E., & Jacobs-Wagner, C. (2014, Dec 4). A constant size extension drives bacterial cell size homeostasis. *Cell, 159*(6), 1433-1446. https://doi.org/10.1016/j.cell.2014.11.022

15. Cesar, S., & Huang, K. C. (2017, Sep 1). Thinking big: the tunability of bacterial cell size. *FEMS Microbiol Rev, 41*(5), 672-678. https://doi.org/10.1093/femsre/fux026

16. Churchward, G., Estiva, E., & Bremer, H. (1981, Mar). Growth rate-dependent control of chromosome replication initiation in Escherichia coli. *J Bacteriol, 145*(3), 1232-1238. https://doi.org/10.1128/jb.145.3.1232-1238.1981

17. Collier, J., Murray, S. R., & Shapiro, L. (2006, 2006/01/25). DnaA couples DNA replication and the expression of two cell cycle master regulators. *The EMBO Journal, 25*(2), 346-356-356. https://doi.org/https://doi.org/10.1038/sj.emboj.7600927

18. Collier, J., Murray, S. R., & Shapiro, L. (2006, Jan 25). DnaA couples DNA replication and the expression of two cell cycle master regulators. *EMBO J, 25*(2), 346-356. https://doi.org/10.1038/sj.emboj.7600927

19. Collier, J., & Shapiro, L. (2009, Sep). Feedback control of DnaA-mediated replication initiation by replisome-associated HdaA protein in Caulobacter. *J Bacteriol, 191*(18), 5706-5716. https://doi.org/10.1128/JB.00525-09

20. Cooper, S., & Helmstetter, C. E. (1968, Feb 14). Chromosome replication and the division cycle of Escherichia coli B/r. *J Mol Biol, 31*(3), 519-540. https://doi.org/10.1016/0022-2836(68)90425-7

21. Cronan, J. E. (2014). A new pathway of exogenous fatty acid incorporation proceeds by a classical phosphoryl transfer reaction. *Molecular microbiology, 92*(2), 217-221.

22. Dalia, A. B., & Weiser, J. N. (2011, Nov 17). Minimization of bacterial size allows for complement evasion and is overcome by the agglutinating effect of antibody. *Cell Host Microbe, 10*(5), 486-496. https://doi.org/10.1016/j.chom.2011.09.009

23. Dion, M. F., Kapoor, M., Sun, Y., Wilson, S., Ryan, J., Vigouroux, A., van Teeffelen, S., Oldenbourg, R., & Garner, E. C. (2019, Aug). Bacillus subtilis cell diameter is determined

by the opposing actions of two distinct cell wall synthetic systems. *Nat Microbiol, 4*(8), 1294-1305. https://doi.org/10.1038/s41564-019-0439-0

24. Donachie, W. D. (1968, Sep 7). Relationship between cell size and time of initiation of DNA replication. *Nature, 219*(5158), 1077-1079. https://doi.org/10.1038/2191077a0

25. Donachie, W. D., Begg, K. J., & Vicente, M. (1976, Nov 25). Cell length, cell growth and cell division. *Nature, 264*(5584), 328-333. https://doi.org/10.1038/264328a0

26. Ducret, A., Quardokus, E. M., & Brun, Y. V. (2016, Jun 20). MicrobeJ, a tool for high throughput bacterial cell detection and quantitative analysis. *Nat Microbiol, 1*(7), 16077. https://doi.org/10.1038/nmicrobiol.2016.77

27. Duderstadt, K. E., & Berger, J. M. (2013, Feb). A structural framework for replication origin opening by AAA+ initiation factors. *Curr Opin Struct Biol, 23*(1), 144-153. https://doi.org/10.1016/j.sbi.2012.11.012

28. Evinger, M., & Agabian, N. (1977, Oct). Envelope-associated nucleoid from Caulobacter crescentus stalked and swarmer cells. *J Bacteriol, 132*(1), 294-301. https://doi.org/10.1128/jb.132.1.294-301.1977

29. Felletti, M., Omnus, D. J., & Jonas, K. (2019, Jul). Regulation of the replication initiator DnaA in Caulobacter crescentus. *Biochim Biophys Acta Gene Regul Mech, 1862*(7), 697-705. https://doi.org/10.1016/j.bbagrm.2018.01.004

30. Felletti, M., Romilly, C., Wagner, E. G. H., & Jonas, K. (2021, Sep 15). A nascent polypeptide sequence modulates DnaA translation elongation in response to nutrient availability. *Elife, 10*. https://doi.org/10.7554/eLife.71611

31. Fernandez-Fernandez, C., Gonzalez, D., & Collier, J. (2011). Regulation of the Activity of the Dual-Function DnaA Protein in Caulobacter crescentus. *PLOS ONE, 6*(10), e26028. https://doi.org/10.1371/journal.pone.0026028

32. Frandi, A., & Collier, J. (2019). Multilayered control of chromosome replication in Caulobacter crescentus. *Biochemical Society Transactions, 47*(1), 187-196. https://doi.org/10.1042/bst20180460

33. Fujikawa, N., Kurumizaka, H., Nureki, O., Terada, T., Shirouzu, M., Katayama, T., & Yokoyama, S. (2003, Apr 15). Structural basis of replication origin recognition by the DnaA protein. *Nucleic Acids Res, 31*(8), 2077-2086. https://doi.org/10.1093/nar/gkg309

34. Glenn, S., Fragasso, A., Lin, W.-H., Papagiannakis, A., Kato, S., & Jacobs-Wagner, C. (2024). Coupling of cell growth modulation to asymmetric division and cell cycle regulation in Caulobacter crescentus. *Proceedings of the National Academy of Sciences, 121*(41), e2406397121. https://doi.org/doi:10.1073/pnas.2406397121

35. Glenn, S., Fragasso, A., Lin, W. H., Papagiannakis, A., Kato, S., & Jacobs-Wagner, C. (2024, Oct 8). Coupling of cell growth modulation to asymmetric division and cell cycle regulation in Caulobacter crescentus. *Proc Natl Acad Sci U S A, 121*(41), e2406397121. https://doi.org/10.1073/pnas.2406397121

36. Goley, E. D., Dye, N. A., Werner, J. N., Gitai, Z., & Shapiro, L. (2010, 2010/09/24/). Imaging-Based Identification of a Critical Regulator of FtsZ Protofilament Curvature in Caulobacter. *Molecular Cell, 39*(6), 975-987. https://doi.org/https://doi.org/10.1016/j.molcel.2010.08.027

37. Gonzalez, D., & Collier, J. (2014, Jul). Effects of (p)ppGpp on the progression of the cell cycle of Caulobacter crescentus. *J Bacteriol, 196*(14), 2514-2525. https://doi.org/10.1128/JB.01575-14

38. Govers, S. K., & Jacobs-Wagner, C. (2020, Oct 5). Caulobacter crescentus: model system extraordinaire. *Curr Biol, 30*(19), R1151-R1158. https://doi.org/10.1016/j.cub.2020.07.033

39. Grant, N. A., Abdel Magid, A., Franklin, J., Dufour, Y., & Lenski, R. E. (2021, Apr 21). Changes in Cell Size and Shape during 50,000 Generations of Experimental Evolution with Escherichia coli. *J Bacteriol, 203*(10). https://doi.org/10.1128/JB.00469-20

40. Haakonsen, D. L., Yuan, A. H., & Laub, M. T. (2015, Nov 1). The bacterial cell cycle regulator GcrA is a sigma70 cofactor that drives gene expression from a subset of methylated promoters. *Genes Dev, 29*(21), 2272-2286. https://doi.org/10.1101/gad.270660.115

41. Hallgren, J., & Jonas, K. (2024, Feb). Nutritional control of bacterial DNA replication. *Curr Opin Microbiol, 77*, 102403. https://doi.org/10.1016/j.mib.2023.102403

42. Hansen, F. G., & Atlung, T. (2018). The DnaA Tale. *Front Microbiol, 9*, 319. https://doi.org/10.3389/fmicb.2018.00319

43. Hansen, F. G., Hansen, E. B., & Atlung, T. (1982). The nucleotide sequence of the dnaA gene promoter and of the adjacent rpmH gene, coding for the ribosomal protein L34, of Escherichia coli. *EMBO J, 1*(9), 1043-1048. https://doi.org/10.1002/j.1460-2075.1982.tb01294.x

44. Harris, L. K., & Theriot, J. A. (2016, Jun 2). Relative Rates of Surface and Volume Synthesis Set Bacterial Cell Size. *Cell, 165*(6), 1479-1492. https://doi.org/10.1016/j.cell.2016.05.045

45. Helmstetter, C., Cooper, S., Pierucci, O., & Revelas, E. (1968). On the bacterial life sequence. *Cold Spring Harb Symp Quant Biol, 33*, 809-822. https://doi.org/10.1101/sqb.1968.033.01.093

46. Hill, N. S., Kadoya, R., Chattoraj, D. K., & Levin, P. A. (2012). Cell size and the initiation of DNA replication in bacteria. *PLoS Genet, 8*(3), e1002549. https://doi.org/10.1371/journal.pgen.1002549

47. Ho, P.-Y., & Amir, A. (2015). Simultaneous regulation of cell size and chromosome replication in bacteria. *Frontiers in microbiology, 6*, 662.

48. Holtzendorff, J., Hung, D., Brende, P., Reisenauer, A., Viollier, P. H., McAdams, H. H., & Shapiro, L. (2004, May 14). Oscillating global regulators control the genetic circuit driving a bacterial cell cycle. *Science, 304*(5673), 983-987. https://doi.org/10.1126/science.1095191

49. Hottes, A. K., Shapiro, L., & McAdams, H. H. (2005). DnaA coordinates replication initiation and cell cycle transcription in Caulobacter crescentus. *Molecular Microbiology, 58*(5), 1340-1353. https://doi.org/https://doi.org/10.1111/j.1365-2958.2005.04912.x

50. Hottes, A. K., Shapiro, L., & McAdams, H. H. (2005, Dec). DnaA coordinates replication initiation and cell cycle transcription in Caulobacter crescentus. *Mol Microbiol, 58*(5), 1340-1353. https://doi.org/10.1111/j.1365-2958.2005.04912.x

51. Ikeda, M., Wachi, M., Jung, H. K., Ishino, F., & Matsuhashi, M. (1991, Feb). The Escherichia coli mraY gene encoding UDP-N-acetylmuramoyl-pentapeptide: undecaprenyl-phosphate phospho-N-acetylmuramoyl-pentapeptide transferase. *J Bacteriol, 173*(3), 1021-1026. https://doi.org/10.1128/jb.173.3.1021-1026.1991

52. Iniesta, A. A., McGrath, P. T., Reisenauer, A., McAdams, H. H., & Shapiro, L. (2006, Jul 18). A phospho-signaling pathway controls the localization and activity of a protease complex critical for bacterial cell cycle progression. *Proc Natl Acad Sci U S A, 103*(29), 10935-10940. https://doi.org/10.1073/pnas.0604554103

53. Irnov, I., Wang, Z., Jannetty, N. D., Bustamante, J. A., Rhee, K. Y., & Jacobs-Wagner, C. (2017). Crosstalk between the tricarboxylic acid cycle and peptidoglycan synthesis in Caulobacter crescentus through the homeostatic control of α-ketoglutarate. *PLOS Genetics, 13*(8), e1006978. https://doi.org/10.1371/journal.pgen.1006978

54. Jensen, R. B., Wang, S. C., & Shapiro, L. (2001, Sep 3). A moving DNA replication factory in Caulobacter crescentus. *EMBO J, 20*(17), 4952-4963. https://doi.org/10.1093/emboj/20.17.4952

55. Jun, S., Si, F., Pugatch, R., & Scott, M. (2018, May). Fundamental principles in bacterial physiology-history, recent progress, and the future with focus on cell size control: a review. *Rep Prog Phys, 81*(5), 056601. https://doi.org/10.1088/1361-6633/aaa628

56. Jutras, B. L., Bowman, A., Brissette, C. A., Adams, C. A., Verma, A., Chenail, A. M., & Stevenson, B. (2012, Jul). EbfC (YbaB) is a new type of bacterial nucleoid-associated

protein and a global regulator of gene expression in the Lyme disease spirochete. *J Bacteriol, 194*(13), 3395-3406. https://doi.org/10.1128/JB.00252-12

57. Kaneda, T. (1991). Iso-and anteiso-fatty acids in bacteria: biosynthesis, function, and taxonomic significance. *Microbiological reviews, 55*(2), 288-302.

58. Katayama, T., Ozaki, S., Keyamura, K., & Fujimitsu, K. (2010). Regulation of the replication cycle: conserved and diverse regulatory systems for DnaA and oriC. *Nature Reviews Microbiology, 8*(3), 163-170.

59. Kelly, A. J., Sackett, M. J., Din, N., Quardokus, E., & Brun, Y. V. (1998, Mar 15). Cell cycle-dependent transcriptional and proteolytic regulation of FtsZ in Caulobacter. *Genes Dev, 12*(6), 880-893. https://doi.org/10.1101/gad.12.6.880

60. Kirkpatrick, C. L., & Viollier, P. H. (2012, Jan). Decoding Caulobacter development. *FEMS Microbiol Rev, 36*(1), 193-205. https://doi.org/10.1111/j.1574-6976.2011.00309.x

61. Kohiyama, M. (2020, Dec). Research on DnaA in the early days. *Res Microbiol, 171*(8), 287-289. https://doi.org/10.1016/j.resmic.2020.11.004

62. Koppes, L. J., Meyer, M., Oonk, H. B., de Jong, M. A., & Nanninga, N. (1980, Sep). Correlation between size and age at different events in the cell division cycle of Escherichia coli. *J Bacteriol, 143*(3), 1241-1252. https://doi.org/10.1128/jb.143.3.1241-1252.1980

63. Krusenstjerna, A. C., Jusufovic, N., Saylor, T. C., & Stevenson, B. (2024, Aug 29). DnaA modulates the gene expression and morphology of the Lyme disease spirochete. *bioRxiv*. https://doi.org/10.1101/2024.06.08.598065

64. Krusenstjerna, A. C., Saylor, T. C., Arnold, W. K., Tucker, J. S., & Stevenson, B. (2023, Jan 26). Borrelia burgdorferi DnaA and the Nucleoid-Associated Protein EbfC Coordinate Expression of the dnaX-ebfC Operon. *J Bacteriol, 205*(1), e0039622. https://doi.org/10.1128/jb.00396-22

65. Lambert, A., Vanhecke, A., Archetti, A., Holden, S., Schaber, F., Pincus, Z., Laub, M. T., Goley, E., & Manley, S. (2018, 2018/06/29/). Constriction Rate Modulation Can Drive Cell Size Control and Homeostasis in C. crescentus. *iScience, 4*, 180-189. https://doi.org/https://doi.org/10.1016/j.isci.2018.05.020

66. Lariviere, P. J., Szwedziak, P., Mahone, C. R., Löwe, J., & Goley, E. D. (2018, Jan). FzlA, an essential regulator of FtsZ filament curvature, controls constriction rate during Caulobacter division. *Mol Microbiol, 107*(2), 180-197. https://doi.org/10.1111/mmi.13876

67. Lenski, R. E., & Travisano, M. (1994, Jul 19). Dynamics of adaptation and diversification: a 10,000-generation experiment with bacterial populations. *Proc Natl Acad Sci U S A, 91*(15), 6808-6814. https://doi.org/10.1073/pnas.91.15.6808

68. Leonard, A. C., & Grimwade, J. E. (2011). Regulation of DnaA assembly and activity: taking directions from the genome. *Annual review of microbiology, 65*(1), 19-35.

69. Levine, A., Vannier, F., Dehbi, M., Henckes, G., & Seror, S. J. (1991, Jun 20). The stringent response blocks DNA replication outside the ori region in Bacillus subtilis and at the origin in Escherichia coli. *J Mol Biol, 219*(4), 605-613. https://doi.org/10.1016/0022-2836(91)90657-r

70. Lobner-Olesen, A., Skarstad, K., Hansen, F. G., von Meyenburg, K., & Boye, E. (1989, Jun 2). The DnaA protein determines the initiation mass of Escherichia coli K-12. *Cell, 57*(5), 881-889. https://doi.org/10.1016/0092-8674(89)90802-7

71. Lord, S. J., Velle, K. B., Mullins, R. D., & Fritz-Laylin, L. K. (2020). SuperPlots: Communicating reproducibility and variability in cell biology. *Journal of Cell Biology, 219*(6). https://doi.org/10.1083/jcb.202001064

72. Maciag, M., Kochanowska, M., Lyzen, R., Wegrzyn, G., & Szalewska-Palasz, A. (2010, Jan). ppGpp inhibits the activity of Escherichia coli DnaG primase. *Plasmid, 63*(1), 61-67. https://doi.org/10.1016/j.plasmid.2009.11.002

73. Mahone, C. R., Payne, I. P., Lyu, Z., McCausland, J. W., Barrows, J. M., Xiao, J., Yang, X., & Goley, E. D. (2024, Feb 5). Integration of cell wall synthesis and chromosome segregation during cell division in Caulobacter. *J Cell Biol, 223*(2). https://doi.org/10.1083/jcb.202211026

74. Marczynski, G. T. (1999, Apr). Chromosome methylation and measurement of faithful, once and only once per cell cycle chromosome replication in Caulobacter crescentus. *J Bacteriol, 181*(7), 1984-1993. https://doi.org/10.1128/JB.181.7.1984-1993.1999

75. Megrian, D., Taib, N., Jaffe, A. L., Banfield, J. F., & Gribaldo, S. (2022, Dec). Ancient origin and constrained evolution of the division and cell wall gene cluster in Bacteria. *Nat Microbiol, 7*(12), 2114-2127. https://doi.org/10.1038/s41564-022-01257-y

76. Menikpurage, I. P., Woo, K., & Mera, P. E. (2021). Transcriptional Activity of the Bacterial Replication Initiator DnaA. *Front Microbiol, 12*, 662317. https://doi.org/10.3389/fmicb.2021.662317

77. Mera, P. E., Kalogeraki, V. S., & Shapiro, L. (2014). Replication initiator DnaA binds at the Caulobacter centromere and enables chromosome segregation. *Proceedings of the National Academy of Sciences, 111*(45), 16100-16105.

78. Messer, W., & Weigel, C. (1997, Apr). DnaA initiator--also a transcription factor. *Mol Microbiol, 24*(1), 1-6. https://doi.org/10.1046/j.1365-2958.1997.3171678.x

79. Messer, W., & Weigel, C. (1997). DnaA initiator—also a transcription factor. *Molecular microbiology, 24*(1), 1-6.

80. Mizushima, T., Sasaki, S., Ohishi, H., Kobayashi, M., Katayama, T., Miki, T., Maeda, M., & Sekimizu, K. (1996, Oct 11). Molecular design of inhibitors of in vitro oriC DNA replication based on the potential to block the ATP binding of DnaA protein. *J Biol Chem, 271*(41), 25178-25183. https://doi.org/10.1074/jbc.271.41.25178

81. Mizushima, T., Takaki, T., Kubota, T., Tsuchiya, T., Miki, T., Katayama, T., & Sekimizu, K. (1998, Aug 14). Site-directed mutational analysis for the ATP binding of DnaA protein. Functions of two conserved amino acids (Lys-178 and Asp-235) located in the ATP-binding domain of DnaA protein in vitro and in vivo. *J Biol Chem, 273*(33), 20847-20851. https://doi.org/10.1074/jbc.273.33.20847

82. Morrison, J. J., & Camberg, J. L. (2024). Building the Bacterial Divisome at the Septum. *Subcell Biochem, 104*, 49-71. https://doi.org/10.1007/978-3-031-58843-3_4

83. Ng, T. W., Ojkic, N., Serbanescu, D., & Banerjee, S. (2024). Differential growth regulates asymmetric size partitioning in Caulobacter crescentus. *Life Science Alliance, 7*(8), e202402591. https://doi.org/10.26508/lsa.202402591

84. Ng, T. W., Ojkic, N., Serbanescu, D., & Banerjee, S. (2024, Aug). Differential growth regulates asymmetric size partitioning in Caulobacter crescentus. *Life Sci Alliance, 7*(8). https://doi.org/10.26508/lsa.202402591

85. Nikolaichik, Y. A., & Donachie, W. D. (2000). Conservation of gene order amongst cell wall and cell division genes in Eubacteria, and ribosomal genes in Eubacteria and Eukaryotic organelles. *Genetica, 108*(1), 1-7. https://doi.org/10.1023/a:1004077806910

86. Olliver, A., Saggioro, C., Herrick, J., & Sclavi, B. (2010, Jun). DnaA-ATP acts as a molecular switch to control levels of ribonucleotide reductase expression in Escherichia coli. *Mol Microbiol, 76*(6), 1555-1571. https://doi.org/10.1111/j.1365-2958.2010.07185.x

87. Sackett, M. J., Kelly, A. J., & Brun, Y. V. (1998, May). Ordered expression of ftsQA and ftsZ during the Caulobacter crescentus cell cycle. *Mol Microbiol, 28*(3), 421-434. https://doi.org/10.1046/j.1365-2958.1998.00753.x

88. Salama, N. R. (2020, Apr). Cell morphology as a virulence determinant: lessons from Helicobacter pylori. *Curr Opin Microbiol, 54*, 11-17. https://doi.org/10.1016/j.mib.2019.12.002

89. Sargent, M. G. (1975, Jul). Control of cell length in Bacillus subtilis. *J Bacteriol, 123*(1), 7-19. https://doi.org/10.1128/jb.123.1.7-19.1975

90. Schaechter, M., Maaloe, O., & Kjeldgaard, N. O. (1958, Dec). Dependency on medium and temperature of cell size and chemical composition during balanced grown of

Salmonella typhimurium. *J Gen Microbiol, 19*(3), 592-606. https://doi.org/10.1099/00221287-19-3-592

91. Schaechter, M., Maaløe, O., & Kjeldgaard, N. O. (1958). Dependency on medium and temperature of cell size and chemical composition during balanced growth of Salmonella typhimurium. *Microbiology, 19*(3), 592-606.

92. Schindelin, J., Arganda-Carreras, I., Frise, E., Kaynig, V., Longair, M., Pietzsch, T., Preibisch, S., Rueden, C., Saalfeld, S., & Schmid, B. (2012). Fiji: an open-source platform for biological-image analysis. *Nature Methods, 9*(7), 676-682.

93. Schindelin, J., Arganda-Carreras, I., Frise, E., Kaynig, V., Longair, M., Pietzsch, T., Preibisch, S., Rueden, C., Saalfeld, S., Schmid, B., Tinevez, J.-Y., White, D. J., Hartenstein, V., Eliceiri, K., Tomancak, P., & Cardona, A. (2012, 2012/07/01). Fiji: an open-source platform for biological-image analysis. *Nature Methods, 9*(7), 676-682. https://doi.org/10.1038/nmeth.2019

94. Schrader, J. M., Li, G.-W., Childers, W. S., Perez, A. M., Weissman, J. S., Shapiro, L., & McAdams, H. H. (2016). Dynamic translation regulation in Caulobacter cell cycle control. *Proceedings of the National Academy of Sciences, 113*(44), E6859-E6867.

95. Schrader, J. M., Li, G. W., Childers, W. S., Perez, A. M., Weissman, J. S., Shapiro, L., & McAdams, H. H. (2016, Nov 1). Dynamic translation regulation in Caulobacter cell cycle control. *Proc Natl Acad Sci U S A, 113*(44), E6859-E6867. https://doi.org/10.1073/pnas.1614795113

96. Schrader, J. M., & Shapiro, L. (2015, Apr 8). Synchronization of Caulobacter crescentus for investigation of the bacterial cell cycle. *J Vis Exp*(98). https://doi.org/10.3791/52633

97. Schwartz, M. A., & Shapiro, L. (2011). An SMC ATPase mutant disrupts chromosome segregation in Caulobacter. *Molecular microbiology, 82*(6), 1359-1374.

98. Sekimizu, K., Bramhill, D., & Kornberg, A. (1987, Jul 17). ATP activates dnaA protein in initiating replication of plasmids bearing the origin of the E. coli chromosome. *Cell, 50*(2), 259-265. https://doi.org/10.1016/0092-8674(87)90221-2

99. Si, F., Le Treut, G., Sauls, J. T., Vadia, S., Levin, P. A., & Jun, S. (2019, Jun 3). Mechanistic Origin of Cell-Size Control and Homeostasis in Bacteria. *Curr Biol, 29*(11), 1760-1770 e1767. https://doi.org/10.1016/j.cub.2019.04.062

100. Si, F., Li, D., Cox, S. E., Sauls, J. T., Azizi, O., Sou, C., Schwartz, A. B., Erickstad, M. J., Jun, Y., & Li, X. (2017). Invariance of initiation mass and predictability of cell size in Escherichia coli. *Current Biology, 27*(9), 1278-1287.

101. Si, F., Li, D., Cox, S. E., Sauls, J. T., Azizi, O., Sou, C., Schwartz, A. B., Erickstad, M. J., Jun, Y., Li, X., & Jun, S. (2017, May 8). Invariance of Initiation Mass and Predictability of

Cell Size in Escherichia coli. *Curr Biol, 27*(9), 1278-1287. https://doi.org/10.1016/j.cub.2017.03.022

102. Sink, R., Barreteau, H., Patin, D., Mengin-Lecreulx, D., Gobec, S., & Blanot, D. (2013, Dec). MurD enzymes: some recent developments. *Biomol Concepts, 4*(6), 539-556. https://doi.org/10.1515/bmc-2013-0024

103. Speck, C., Weigel, C., & Messer, W. (1999, Nov 1). ATP- and ADP-dnaA protein, a molecular switch in gene regulation. *EMBO J, 18*(21), 6169-6176. https://doi.org/10.1093/emboj/18.21.6169

104. Srivatsan, A., & Wang, J. D. (2008, Apr). Control of bacterial transcription, translation and replication by (p)ppGpp. *Curr Opin Microbiol, 11*(2), 100-105. https://doi.org/10.1016/j.mib.2008.02.001

105. Stephens, C., Christen, B., Watanabe, K., Fuchs, T., & Jenal, U. (2007). Regulation of d-Xylose Metabolism in Caulobacter crescentus by a LacI-Type Repressor. *Journal of Bacteriology, 189*(24), 8828-8834. https://doi.org/doi:10.1128/jb.01342-07

106. Stove, J. L., & Stanier, R. Y. (1962, 1962/12/01). Cellular Differentiation in Stalked Bacteria. *Nature, 196*(4860), 1189-1192. https://doi.org/10.1038/1961189a0

107. Sundararajan, K., Miguel, A., Desmarais, S. M., Meier, E. L., Casey Huang, K., & Goley, E. D. (2015, 2015/06/23). The bacterial tubulin FtsZ requires its intrinsically disordered linker to direct robust cell wall construction. *Nature Communications, 6*(1), 7281. https://doi.org/10.1038/ncomms8281

108. Taylor, J. A., Sichel, S. R., & Salama, N. R. (2019, Sep 8). Bent Bacteria: A Comparison of Cell Shape Mechanisms in Proteobacteria. *Annu Rev Microbiol, 73*, 457-480. https://doi.org/10.1146/annurev-micro-020518-115919

109. Thanbichler, M., Iniesta, A. A., & Shapiro, L. (2007). A comprehensive set of plasmids for vanillate- and xylose-inducible gene expression in Caulobacter crescentus. *Nucleic Acids Research, 35*(20), e137-e137. https://doi.org/10.1093/nar/gkm818

110. Thanbichler, M., & Shapiro, L. (2006, 08/01). MipZ, a Spatial Regulator Coordinating Chromosome Segregation with Cell Division in Caulobacter. *Cell, 126*, 147-162. https://doi.org/10.1016/j.cell.2006.05.038

111. Toro, E., Hong, S. H., McAdams, H. H., & Shapiro, L. (2008, Oct 7). Caulobacter requires a dedicated mechanism to initiate chromosome segregation. *Proc Natl Acad Sci U S A, 105*(40), 15435-15440. https://doi.org/10.1073/pnas.0807448105

112. Tozawa, Y., & Nomura, Y. (2011, Sep). Signalling by the global regulatory molecule ppGpp in bacteria and chloroplasts of land plants. *Plant Biol (Stuttg), 13*(5), 699-709. https://doi.org/10.1111/j.1438-8677.2011.00484.x

113. Traxler, M. F., Summers, S. M., Nguyen, H. T., Zacharia, V. M., Hightower, G. A., Smith, J. T., & Conway, T. (2008, Jun). The global, ppGpp-mediated stringent response to amino acid starvation in Escherichia coli. *Mol Microbiol, 68*(5), 1128-1148. https://doi.org/10.1111/j.1365-2958.2008.06229.x

114. Tsai, J.-W., & Alley, M. R. K. (2001). Proteolysis of the Caulobacter McpA Chemoreceptor Is Cell Cycle Regulated by a ClpX-Dependent Pathway. *Journal of Bacteriology, 183*, 5001 - 5007.

115. Typas, A., Banzhaf, M., Gross, C. A., & Vollmer, W. (2012, 2012/02/01). From the regulation of peptidoglycan synthesis to bacterial growth and morphology. *Nature Reviews Microbiology, 10*(2), 123-136. https://doi.org/10.1038/nrmicro2677

116. Vadia, S., Tse, J. L., Lucena, R., Yang, Z., Kellogg, D. R., Wang, J. D., & Levin, P. A. (2017, Jun 19). Fatty Acid Availability Sets Cell Envelope Capacity and Dictates Microbial Cell Size. *Curr Biol, 27*(12), 1757-1767.e1755. https://doi.org/10.1016/j.cub.2017.05.076

117. Washington, T. A., Smith, J. L., & Grossman, A. D. (2017). Genetic networks controlled by the bacterial replication initiator and transcription factor DnaA in Bacillus subtilis. *Molecular microbiology, 106*(1), 109-128.

118. Weart, R. B., Lee, A. H., Chien, A. C., Haeusser, D. P., Hill, N. S., & Levin, P. A. (2007, Jul 27). A metabolic sensor governing cell size in bacteria. *Cell, 130*(2), 335-347. https://doi.org/10.1016/j.cell.2007.05.043

119. Weart, R. B., & Levin, P. A. (2003, May). Growth rate-dependent regulation of medial FtsZ ring formation. *J Bacteriol, 185*(9), 2826-2834. https://doi.org/10.1128/JB.185.9.2826-2834.2003

120. Wells, D. H., & Long, S. R. (2002, Mar). The Sinorhizobium meliloti stringent response affects multiple aspects of symbiosis. *Mol Microbiol, 43*(5), 1115-1127. https://doi.org/10.1046/j.1365-2958.2002.02826.x

121. Werner, J. N., Shi, H., Hsin, J., Huang, K. C., Gitai, Z., & Klein, E. A. (2020, Aug 4). AimB Is a Small Protein Regulator of Cell Size and MreB Assembly. *Biophys J, 119*(3), 593-604. https://doi.org/10.1016/j.bpj.2020.04.029

122. Westfall, C. S., & Levin, P. A. (2017, Sep 8). Bacterial Cell Size: Multifactorial and Multifaceted. *Annu Rev Microbiol, 71*, 499-517. https://doi.org/10.1146/annurev-micro-090816-093803

123. Williams, B., Bhat, N., Chien, P., & Shapiro, L. (2014, Sep). ClpXP and ClpAP proteolytic activity on divisome substrates is differentially regulated following the Caulobacter asymmetric cell division. *Mol Microbiol, 93*(5), 853-866. https://doi.org/10.1111/mmi.12698

124. Willis, L., & Huang, K. (2017, 08/14). Sizing up the bacterial cell cycle. *Nature Reviews Microbiology, 15*. https://doi.org/10.1038/nrmicro.2017.79

125. Wold, S., Skarstad, K., Steen, H. B., Stokke, T., & Boye, E. (1994, May 1). The initiation mass for DNA replication in Escherichia coli K-12 is dependent on growth rate. *EMBO J, 13*(9), 2097-2102. https://doi.org/10.1002/j.1460-2075.1994.tb06485.x

126. Woldringh, C. L., Grover, N. B., Rosenberger, R. F., & Zaritsky, A. (1980, Oct 7). Dimensional rearrangement of rod-shaped bacteria following nutritional shift-up. II. Experiments with Escherichia coli B/r. *J Theor Biol, 86*(3), 441-454. https://doi.org/10.1016/0022-5193(80)90344-6

127. Yao, Z., Davis, R. M., Kishony, R., Kahne, D., & Ruiz, N. (2012). Regulation of cell size in response to nutrient availability by fatty acid biosynthesis in Escherichia coli. *Proceedings of the National Academy of Sciences, 109*(38), E2561-E2568.

128. Yoshikawa, H., O'Sullivan, A., & Sueoka, N. (1964, Oct). Sequential Replication of the Bacillus Subtilis Chromosome. 3. Regulation of Initiation. *Proc Natl Acad Sci U S A, 52*(4), 973-980. https://doi.org/10.1073/pnas.52.4.973

129. Young, K. D. (2006, Sep). The selective value of bacterial shape. *Microbiol Mol Biol Rev, 70*(3), 660-703. https://doi.org/10.1128/mmbr.00001-06

130. Zheng, H., Bai, Y., Jiang, M., Tokuyasu, T. A., Huang, X., Zhong, F., Wu, Y., Fu, X., Kleckner, N., Hwa, T., & Liu, C. (2020, Aug). General quantitative relations linking cell growth and the cell cycle in Escherichia coli. *Nat Microbiol, 5*(8), 995-1001. https://doi.org/10.1038/s41564-020-0717-x

131. Zheng, H., Ho, P. Y., Jiang, M., Tang, B., Liu, W., Li, D., Yu, X., Kleckner, N. E., Amir, A., & Liu, C. (2016, Dec 27). Interrogating the Escherichia coli cell cycle by cell dimension perturbations. *Proc Natl Acad Sci U S A, 113*(52), 15000-15005. https://doi.org/10.1073/pnas.1617932114

Figure 1

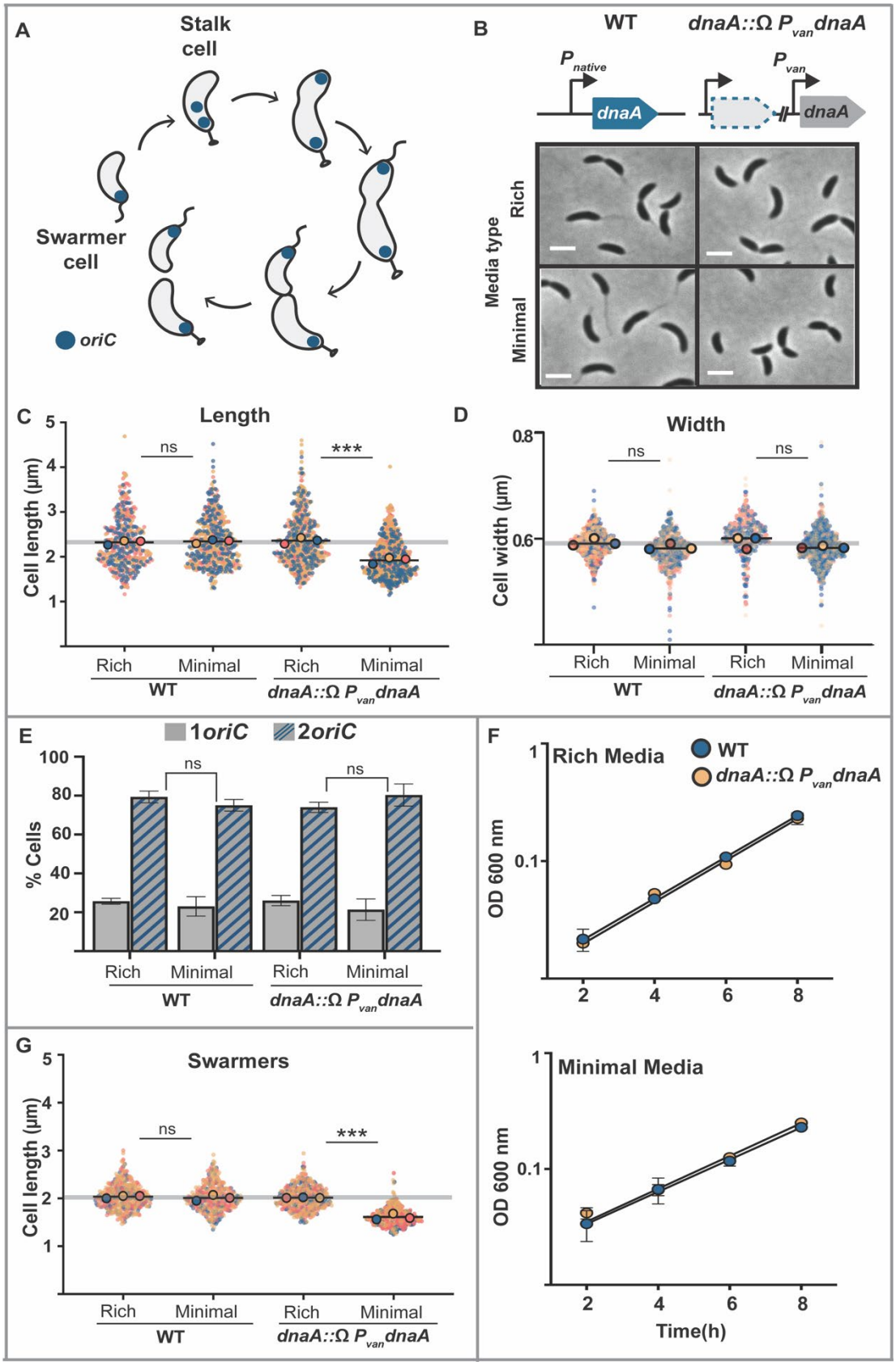

Figure 2

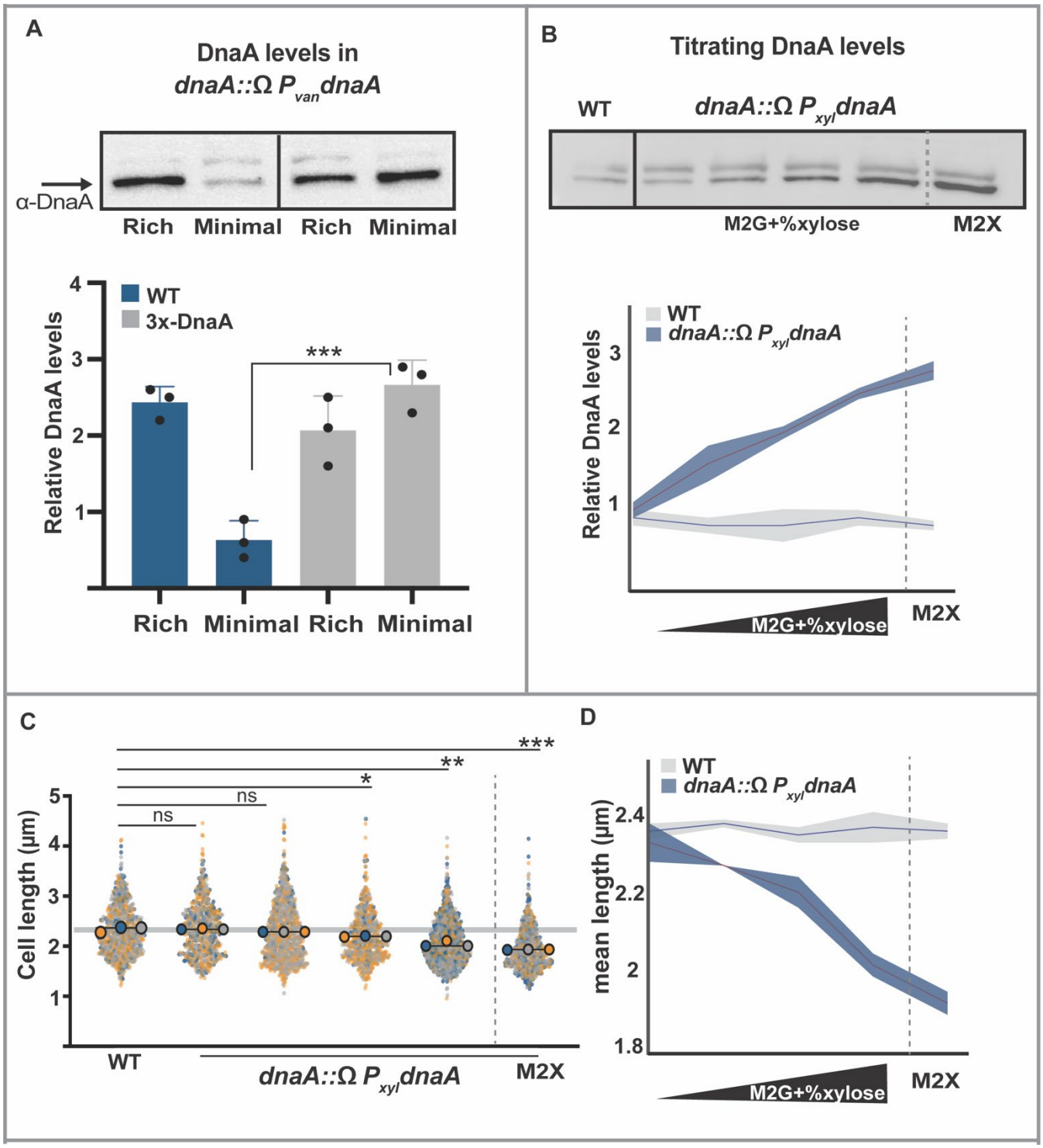

Figure 3

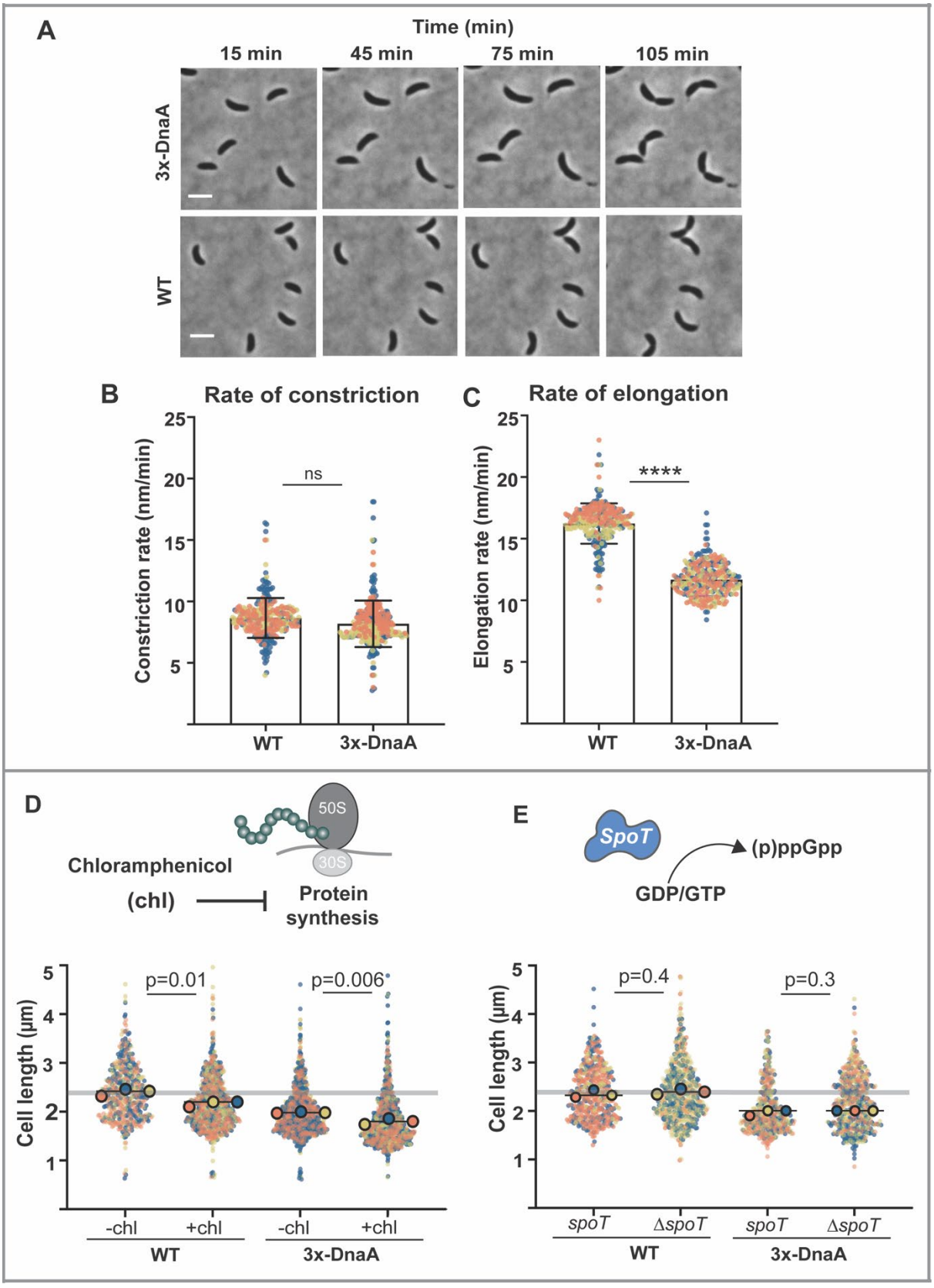

Figure 4

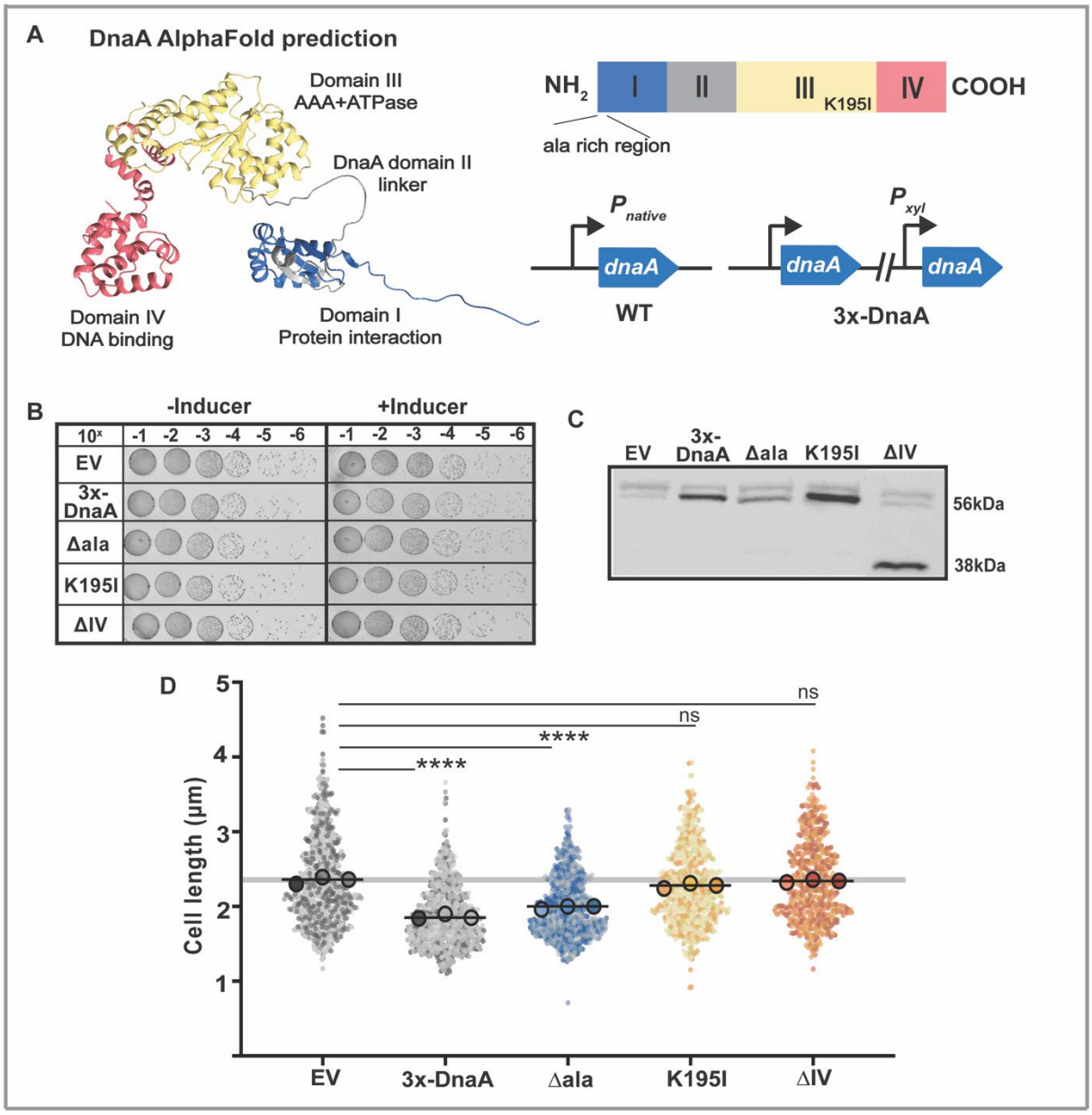

Figure 5

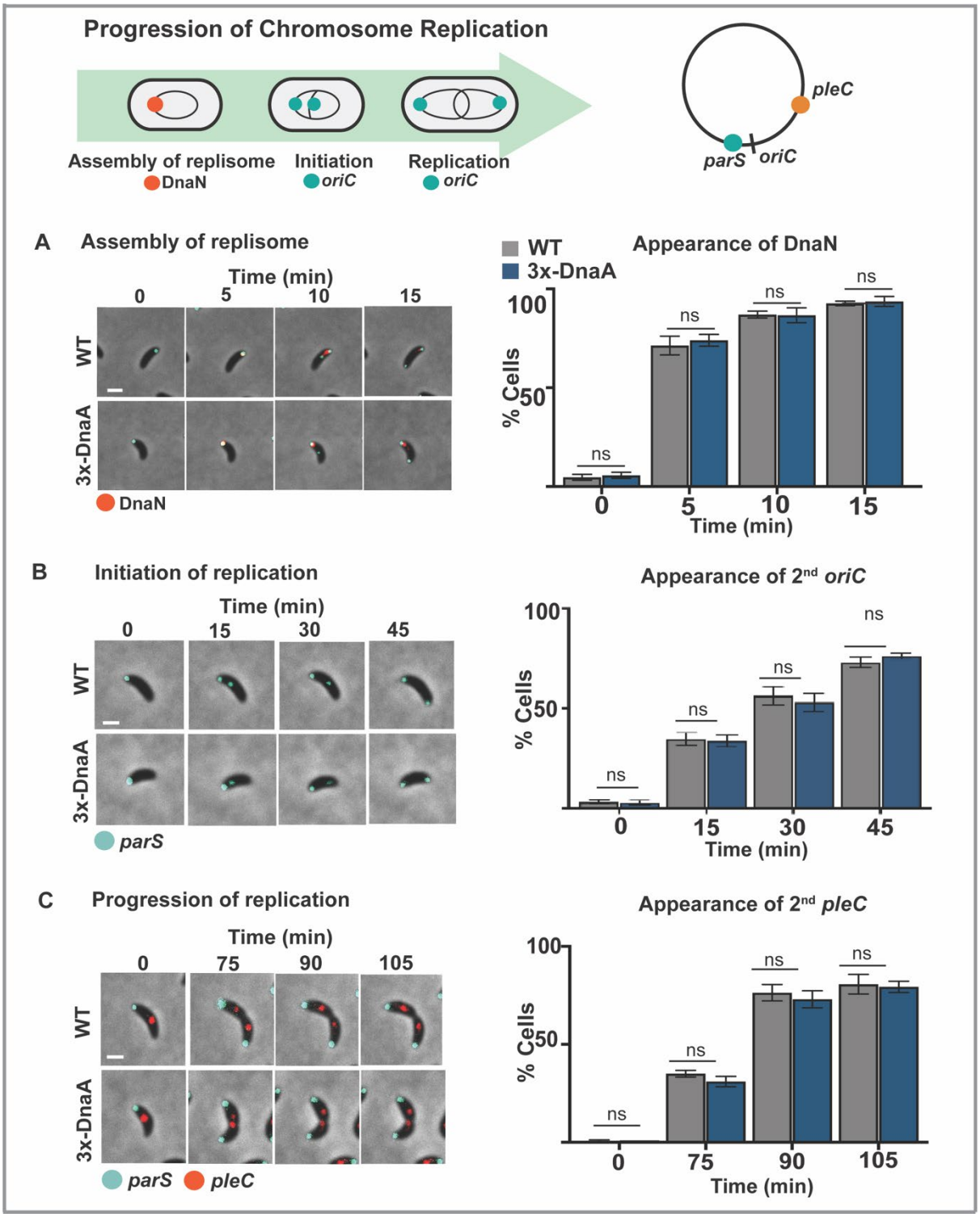

Figure 6

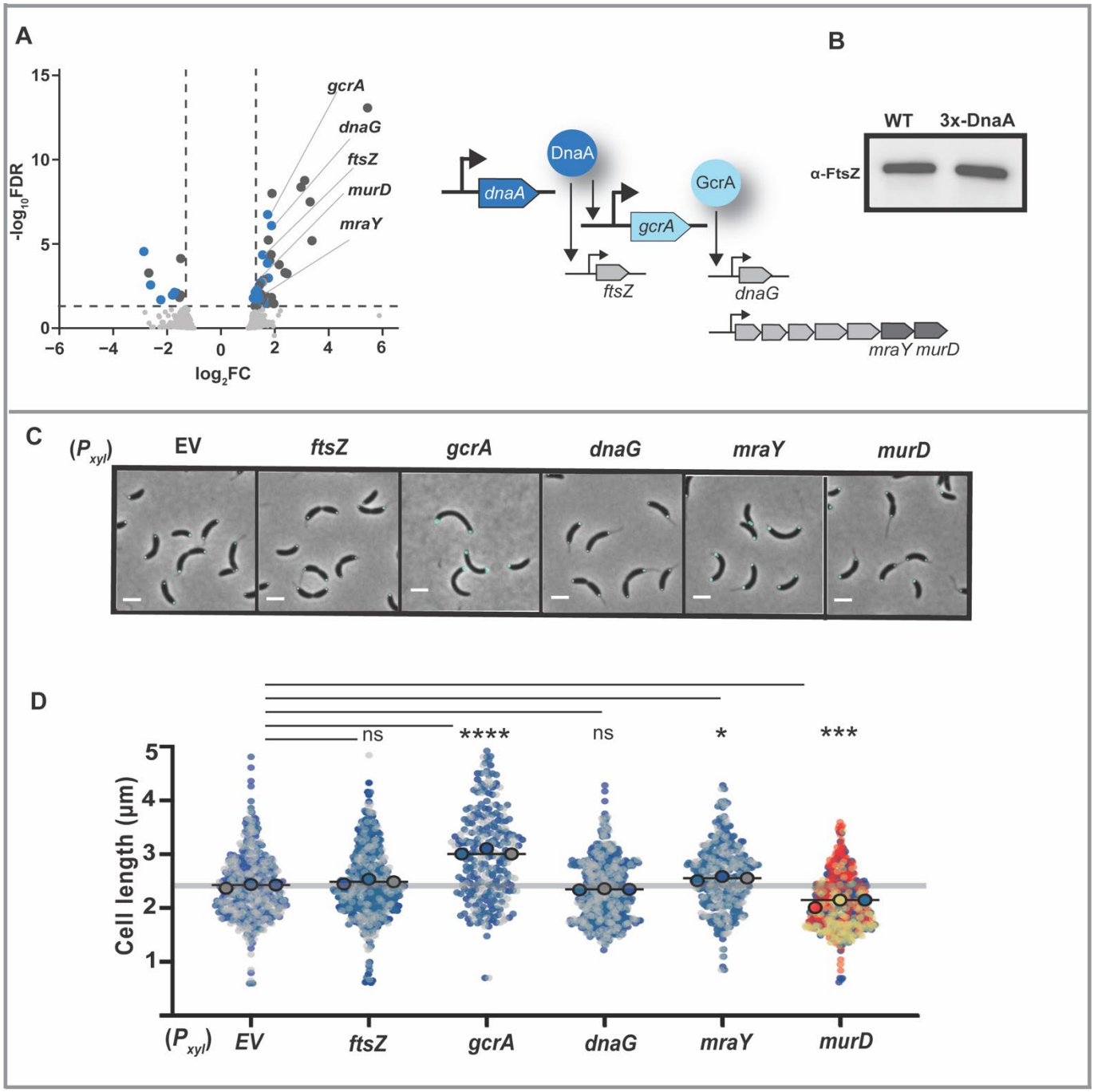

Figure 7

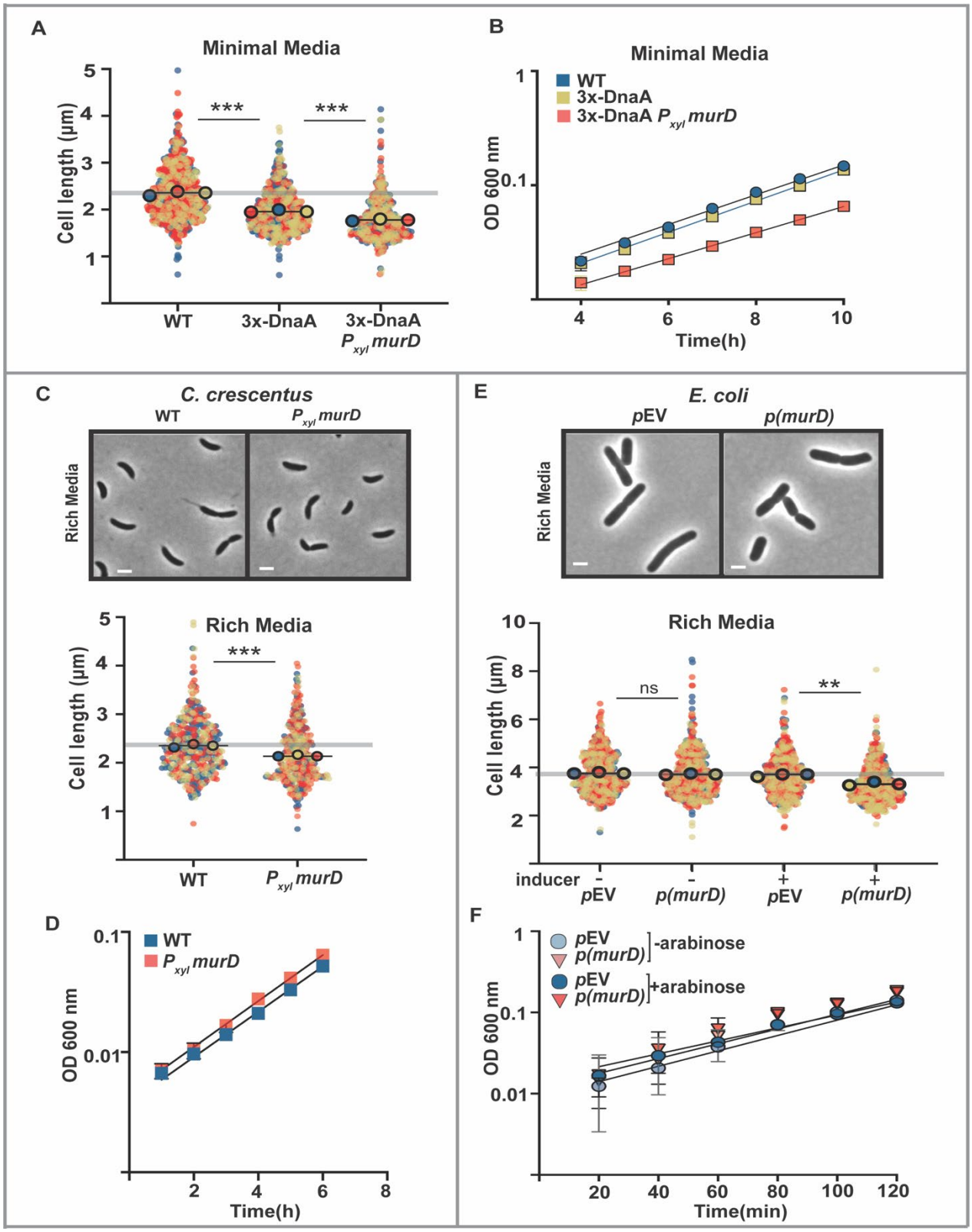

Table 1. RNA-seq data 3x-DnaA vs. DnaA-K195I

Gene ID	Symbol	FC	FDR	Description
CCNA_02793	*NA*	3.3	1.60E-10	S9 family peptidase
CCNA_02792	*NA*	3.1	7.27E-12	TonB-dependent outer membrane receptor
CCNA_03227	*NA*	1.9	1.52E-02	TonB-dependent receptor
CCNA_03144	***dnaG***	1.8	7.54E-07	DNA primase
CCNA_02328	***gcrA***	1.8	3.56E-07	cell cycle sigma 70 cofactor GcrA
CCNA_02891	*NA*	1.7	1.21E-02	GanA-family beta-galactosidase
CCNA_02976	*NA*	1.7	3.46E-02	MCP-signal associated domain protein
CCNA_02640	***mraY***	1.6	1.63E-02	phospho-N-acetylmuramoyl-pentapeptide-transferase
CCNA_03270	*NA*	1.6	3.53E-02	AsnC-family transcriptional regulator
CCNA_02902	*NA*	1.5	1.89E-03	xylan alpha-1,2-glucuronosidase
CCNA_01485	*NA*	1.5	2.18E-02	aldose 1-epimerase
CCNA_01486	*NA*	1.5	1.93E-02	GguC-family protein
CCNA_02639	***murD***	1.5	1.99E-03	UDP-N-acetylmuramoylalanine--D-glutamate ligase
CCNA_02623	***ftsZ***	1.5	6.00E-05	cell division protein FtsZ
CCNA_01003	*fliO*	1.5	3.48E-02	flagellar biosynthesis protein FliO
CCNA_01979	*lexA*	1.5	3.46E-02	LexA repressor
CCNA_01116	*divJ*	1.5	9.31E-03	histidine protein kinase DivJ
CCNA_01489	*abfA*	1.5	3.37E-02	alpha-L-arabinofuranosidase
CCNA_03105	*NA*	-1.5	1.09E-02	DnaJ domain protein
CCNA_02814	*NA*	-1.5	1.52E-02	transposase
CCNA_03426	*NA*	-1.8	1.09E-02	MarR family repressor protein
CCNA_01247	*NA*	-2.6	2.74E-03	CESA-like glycosyltransferase
CCNA_03231	*relB-4*	-2.9	2.85E-05	anti-toxin protein relB-4